ARTICLE COVER SHEET

LWW_NEN-FLA

SERVER-BASED

Template version : 4.2
Revised: 03/08/2013

Article : NEN14260
Creator :
Date : 2/13/2015
Time : 10:13
Number of Pages (including this page) : 28

J Neuropathol Exp Neurol
Vol. 74, No. 4
April 2015
pp. 00–00

ORIGINAL ARTICLE

Neuroinflammatory Signals in Alzheimer Disease and APP/PS1 Transgenic Mice: Correlations With Plaques, Tangles, and Oligomeric Species

Irene López-González, MSc, Agatha Schlüter, PhD, Ester Aso, PhD, Paula Garcia-Esparcia, MSc, Belen Ansoleaga, MSc, Franc LLorens, PhD, Margarita Carmona, Tech, Jesús Moreno, Tech, Andrea Fuso, MD, PhD, Manuel Portero-Otin, MD, PhD, Reinald Pamplona, MD, PhD, Aurora Pujol, MD, PhD, and Isidre Ferrer, MD, PhD

Abstract

To understand neuroinflammation-related gene regulation during normal aging and in sporadic Alzheimer disease (sAD), we performed functional genomics analysis and analyzed messenger RNA (mRNA) expression by quantitative reverse transcription–polymerase chain reaction of 22 genes involved in neuroinflammation-like responses in the cerebral cortex of wild-type and APP/PS1 transgenic mice. For direct comparisons, mRNA expression of 18 of the same genes was then analyzed in the entorhinal cortex, orbitofrontal cortex, and frontal cortex area 8 of middle-aged human subjects lacking Alzheimer disease–related pathology and in older subjects with sAD pathology covering Stages I–II/0(A), III–IV/A–B, and V–VI/C of Braak and Braak classification. Modifications of cytokine and immune mediator mRNA expression were found with normal aging in wild-type mice and in middle-aged individuals and patients with early stages of sAD-related pathology; these were accompanied by increased protein expression of certain mediators in ramified microglia. In APP/PS1 mice, inflammatory changes coincided with β-amyloid (Aβ) deposition; increased levels of soluble oligomers paralleled the modified mRNA expression of cytokines and mediators in wild-type mice. In patients with sAD, regulation was stage- and region-dependent and not merely acceleration and exacerbation of mRNA regulation with aging. Gene regulation was also not related to hyperphosphorylated tau deposition in neurofibrillary tangles, Aβ plaque burden, concentration of Aβ1–40 (Aβ40) and Aβ1–42 (Aβ42), or fibrillar Aβ linked to membranes but rather to increased levels of soluble oligomers. Thus, species differences and region- and stage-dependent inflammatory responses in sAD, particularly at the initial stages, indicate the need to identify new anti-inflammatory compounds with specific molecular therapeutic targets.

Key Words: Beta-amyloid, Cytokines, Genomics, Neuroinflammation, Sporadic Alzheimer disease, Tau.

AQ1 From the Institut de Neuropatologia, Institut d'Investigació Biomèdica de Bellvitge–Hospital Universitari de Bellvitge (IL-G, EA, PG-E, BA, FL, MC, JM, AP, IF); Universitat de Barcelona (IF); and Neurometabolic Diseases Laboratory, Institut d'Investigació Biomèdica de Bellvitge (AS, AP), Hospitalet de Llobregat; Catalan Institution for Research and Advanced Studies (AP), Barcelona; Centro de Investigación Biomédica en Red de Enfermedades Neurodegenerativas (IF) and Center for Biomedical Research on Rare Diseases (AS, AP), Madrid; and Department of Experimental Medicine, University of Lleida–Biomedical Research Institute of Lleida, Lleida (MP-O, RP), Spain; and Section Neuroscience, Department of Psychology, Sapienza University of Rome (AF); and European Center for Brain Research/IRCCS Santa Lucia Foundation (AF), Rome, Italy.

Send correspondence and reprint requests to: Isidre Ferrer, MD, PhD, Institut de Neuropatologia, Servei Anatomia Patologica, Hospital Universitari de Bellvitge, Carrer Feixa Llarga sn, Hospitalet de Llobregat, Barcelona 08907, Spain; E-mail: 8082ifa@gmail.com

AQ2 This study was funded by the Seventh Framework Program of the European Commission (Grant No. 278486 [DEVELAGE project] to Isidre Ferrer and Andrea Fuso) and by the Spanish Ministry of Health, Instituto Carlos III (Fondo de Investigación Sanitaria [FIS] PI1100968, FIS PI14/00757, and CIBERNED project BESAD-P to Isidre Ferrer; FIS PI 11/1532 to Manuel Portero-Otin; and Spanish Ministry of Economy and Competitiveness Grant Nos. BFU2009-11879/BFI and PI1300584 to Reinald Pamplona). Agatha Schlüter was supported by FIS ECA07/055.

The authors declare no conflicts of interests.

Supplemental digital content is available for this article. Direct URL citations appear in the printed text and are provided in the HTML and PDF versions of this article on the journal's Web site (www.jneuropath.com).

INTRODUCTION

Alzheimer disease (AD) is a neurodegenerative disorder characterized by extracellular deposits of fibrillar β-amyloid (Aβ) in the brain parenchyma (forming senile plaques) and around cerebral blood vessels (giving rise to Aβ angiopathy) and by intraneuronal deposits of hyperphosphorylated, abnormally conformed, and truncated tau, comprising neurofibrillary tangles (NFTs), dystrophic neurites, and neuropil threads (1). A small minority of patients experience early-onset familial AD linked to mutations of the genes encoding Aβ precursor protein (*APP*), presenilin 1 (*PSN1*), and presenilin 2 (*PSN2*) (2). Most AD patients have late-onset familial AD, which develops as sporadic AD (sAD); possible combinations of low-penetrance genetic and environmental factors may be involved in sAD pathogenesis (2).

In sAD, early abnormal tau deposition appears in certain brainstem nuclei, followed by the entorhinal cortex and olfactory bulb and tracts; later, it extends to the hippocampal complex, basal forebrain, and limbic system, and eventually to the whole cerebral cortex and other regions (3–7). Systematic anatomic studies have allowed categorization of the stages of

disease progression based on accumulation of brain lesions. Braak and Braak Stages I–II are manifested by NFTs in the olfactory bulb and tracts, transentorhinal cortex, and entorhinal cortex, followed by initial involvement of the CA1 region. Stages III–IV augment the number of NFTs in these regions and extend NFTs to the whole CA1 region of the hippocampus, subiculum, temporal cortex, and magnocellular nuclei of the basal forebrain, including Meynert nucleus, amygdala, anterodorsal thalamic nuclei, and tuberomammillary nucleus. At Stages V–VI, in addition to increased severity in affected areas, cortical association areas, including the frontal and parietal cortices, claustrum, reticular nuclei of the thalamus, and, finally, primary sensory areas compromising the primary visual cortex, are involved (3, 5, 6). Beta-amyloid plaques first appear in the neocortex and then progress to practically the whole cerebral cortex, diencephalic nuclei, and, lastly, the cerebellum (3, 5, 8). Regarding senile plaques, Braak and Braak Stage A is characterized by plaques in the neocortex, particularly the orbitofrontal and temporal cortices; Stage B involves, in addition, the association cortices; and Stage C, the primary somatosensory and motor cortical areas (3, 5).

Importantly, cognitive impairment clinically categorized as mild or moderate may occur at Stages III–IV, whereas dementia can appear in individuals with AD pathology at Stages V–VI (9–11). The time between the first appearance of AD-related pathology and the development of cognitive decline and dementia has been estimated to be several decades in those individuals in whom dementia eventually occurs (12). It is worth stressing that AD Stages I–II are present in approximately 85% of individuals aged 65 years (4, 5, 13). Therefore, some degree of neuropathologic change can be considered common and relatively well tolerated, perhaps for a long period; such changes may have devastating effects once thresholds are crossed (13). These facts highlight the need to gain information about the early clinically silent stages of the neurodegenerative process with the aim of understanding early pathogenic mechanisms and identifying possible targets for therapeutic intervention (13–15).

In addition to these pathologic hallmarks, multiple alterations converge in the pathogenesis of AD. Mitochondrial functional defects, increased production of oxidative and nitrosative reactive species, and damage to enzymes involved in energy metabolism cause nerve cell exhaustion (16–18). Altered lipid composition of membranes, particularly lipid rafts (19), and altered production of trophic factors, neurotransmitters, and neuromodulators, together with impaired function of degradation pathways such as those related to cytoplasmic proteolysis, autophagy, and the ubiquitin-proteasome system, also play crucial roles (13, 15, 20, 21).

Inflammation-like responses are common in many neurodegenerative diseases, and chronic neuroinflammation characterized by activated microglia, together with a plethora of upregulated cytokines and mediators of immune response, is harmful to the CNS (22, 23). This assumption is based on particular characteristics of the CNS, where many molecules that are commonly expressed in the systemic immune system are synthesized by microglia, astrocytes, and neurons (14, 22–26). Hundreds of studies have assessed aspects of neuroinflammation in AD, particularly response to and clearance of Aβ (14, 23–39). Similar changes are also well known in AD-related mouse models (40, 41). Microglia are considered the main conductor of neuroinflammation; involvement of neurons and astrocytes further suggests a complex cytokine cycle with deleterious consequences (14, 24–26, 42, 43). In addition to the evidence that neuroinflammation and cell damage are linked to advanced stages of neurodegenerative diseases, including AD, microglia may act as modulators of various neuronal activities and functions that do not necessarily lead to destructive outcomes. Increased expression of certain cytokines and inflammatory mediators may, in certain settings, be beneficial (44–48). As a working hypothesis, inflammatory responses (if present) at the first stages of AD-related pathology might be beneficial as defense from putative damaging toxic molecules.

Despite important achievements in middle and advanced stages of sAD and in related animal models, a comprehensive side-by-side transcriptomewide analysis addressing gene regulation of brain inflammatory responses with age, initial stages of AD-related pathology, and possible regional differences during these early stages is necessary to have a longitudinal and regional picture of the pathogenetic process. Cytokines in the middle temporal cortex and cerebellum are more mobilized and implicated in the latter AD stages than in the developmental course of AD pathology (49), but little is known about different regions at different stages of AD-related pathology. Modifications in the morphology of microglia have been identified with aging and at the first stages of AD-related pathology, however, thus supporting the idea that such changes respond to particular, currently unidentified stimuli and that these cells are probably the source of mediators of intrinsic inflammatory responses (50, 51). Consequently, a deeper understanding of neuroinflammation-related gene regulation during normal aging and at all stages of AD is of utmost importance (14, 52, 53). In the same line, although transgenic models have been widely used to evaluate neuroinflammation and to test anti-inflammatory therapeutic agents (54), a comparison of the messenger RNA (mRNA) expressions of cytokines and mediators of the immune system between sAD and AD-related transgenic models is needed because pathogenic mechanisms in AD models may be different from those in human sAD—in part because most AD-related transgenic mice are produced by expressing mutated human genes that are causative of early-onset familial AD and these animals only exhibit certain aspects of AD pathology such as Aβ plaques but not NFTs. Moreover, there are obvious species differences in gene expression. AQ2

Therefore, the present study first used functional genomics to characterize regulation of cytokine and inflammatory response mediator genes in the cerebral cortex of wild-type (WT) and APP/PS1 transgenic mice. This was followed by a validation analysis of mRNA expression by quantitative reverse transcription (RT)–polymerase chain reaction (PCR) of 22 genes involved in neuroinflammation-like responses. Then, mRNA expression of 18 genes corresponding to cytokines and mediators of the immune system was analyzed in the entorhinal cortex, orbitofrontal cortex, and frontal cortex area 8 of middle-aged (MA) patients who did not have AD-related pathology and older subjects with a range of sAD pathologies. The selection of these genes in human brains was based on the fact that they encode key cytokines, receptors, and mediators of immune responses and because these are the same genes analyzed in

APP/PS1 transgenic mice, thereby facilitating comparative gene expression profiles between sAD and the mouse model. Study of gene expression profiles was followed by analysis of the protein expression of selected mediators, by Western blot analysis in the cerebral cortex of mice and frontal cortex area 8 of humans and by immunohistochemistry in humans, to gain understanding of gene regulation and translation into corresponding proteins at the early stages of sAD-related pathology. Beta-amyloid plaque burden, concentrations of Aβ (Aβ1–40 [Aβ40] and Aβ1–42 [Aβ42]), levels of membrane-bound Aβ, and levels of soluble oligomers were then examined in the same regions and stages to identify any relationships between these Aβ species and expression of genes involved in neuroinflammation-like responses with normal aging, at the first stages of sAD, and during neurodegenerative progression.

MATERIALS AND METHODS

Animals

Experiments were carried out on APP/PS1 mice and WT littermates aged 3, 6, 12, and 20/22 months. The generation of mice expressing a chimeric mouse/human amyloid precursor protein (APPswe) and a human *PSN1* (PS1dE9) has been described (55). In our colony, APP/PS1 transgenic mice developed a few Aβ plaques in the cerebral cortex at the age of 3 months and began to have deficits in learning and memory at the age of 6 months. At this time, the number of Aβ plaques, as revealed by antibodies recognizing human Aβ, rapidly increased in the cerebral cortex (56). Animals were maintained under standard animal housing conditions in a 12-hour dark-light cycle with free access to food and water. Animal care procedures were conducted according to ethical guidelines (European Communities Council Directive 86/609/EEC) and approved by the local ethics committee. None of the animals exhibited systemic disease. APP/PS1 and WT male mice were aged 3, 6, 12, and 20/22 months (7–11 mice for each phenotype and period; total number of animals, 62).

Human Cases

Human brain tissue was obtained from the Institute of Neuropathology Brain Bank (HUB-ICO-IDIBELL Biobank, Barcelona, Spain) and Clinic Hospital-IDIBAPS Biobank (Barcelona, Spain) following the guidelines of Spanish legislation and of the local ethics committee.

One hemisphere was immediately cut into 1-cm-thick coronal sections, and selected areas of the encephalon were rapidly dissected, frozen on metal plates over dry ice, placed in individual air-tight plastic bags, numbered with water-resistant ink, and stored at −80°C. The other hemisphere was fixed by immersion in 4% buffered formalin for 3 weeks for morphologic studies. Selected fresh samples of frontal cortex area 8 and entorhinal cortex were immediately fixed with 4% paraformaldehyde for 24 hours, cryoprotected with 30% sucrose, and frozen and stored at −80°C until use.

Brain samples from 114 cases were used in the present study (67 men and 47 women). Categorization of the inclusion of cases in the present work was based solely on neuropathologic data; correlation of present data with other classifications was not the purpose of the present study. Neuropathologic categorization was performed according to the Braak and Braak classification adapted for paraffin sections (3, 57). No early-onset familial AD cases were included. Cases with associated neurodegenerative process (i.e. Lewy pathology and argyrophilic grain pathology) and metabolic syndrome were not included. Importantly, cases with systemic inflammatory (including autoimmune diseases) and infectious diseases were rejected. Special care was also taken to not include cases with prolonged agonal state (patients subjected to intensive care or experiencing hypoxia). Only cases with minor changes consistent with small blood vessel disease were acceptable for the present study. Middle-aged subjects were those with no clinical or neuropathologic lesions, including the first stages of AD-related pathology; these cases were used for baseline information on gene expression in individuals aged between 39 and 85 years who had no AD-related pathology. A summary of cases analyzed is shown in Table 1. T1

Cases and regions examined are summarized as follows: entorhinal cortex area 28: 11 AD Stages I–II (mean [SD], 77 [3.1] years), 13 AD Stages III–IV (79 [1.7] years), 15 AD Stages V–VI (81 [2.8] years), and 7 MA cases (53 [2.7] years); orbitofrontal cortex: 10 AD Stages I–II (75 [3.2] years), 15 AD Stages III–IV (80 [1.9] years), 6 AD Stages V–VI (77 [5.0] years), and 11 MA cases (53 [3.7] years); and frontal cortex area 8: 11 AD Stages I–II (74 [2.8] years), 9 AD Stages III–IV (79 [3.0] years), 20 AD Stages V–VI (81 [1.6] years), and 15 MA cases (63 [3] years). Importantly, most cases at Braak and Braak Stages I and II had no Aβ deposits, although a small number of cases had a few scattered diffuse Aβ plaques mainly in the temporal and orbitofrontal cortices (Stages 0 and A of Braak and Braak classification); cases at Stages III–IV had variable amounts of diffuse plaques in the cerebral cortex (Stages A and B of Braak and Braak classification); finally, cases at Stages V–VI had abundant neuritic plaques in the cerebral cortex (Stage C of Braak and Braak classification). Not all regions were available in every case, thus accounting for the large number of individual samples used to encompass the AQ2

TABLE 1. Summary of Cases

Diagnosis	No. Cases	Age, Mean (Range), Years	Postmortem Delay Range
Middle age with no AD pathology	30 (9 female, 21 male)	58.3 (39–85)	2 hours 15 minutes–17 hours 15 minutes
AD I–II/0(A)	22 (6 female, 16 male)	73 (55–86)	2 hours 55 minutes–16 hours 45 minutes
AD III–IV/A–B	28 (15 female, 13 male)	80.5 (67–99)	2 hours 30 minutes–13 hours 30 minutes
AD V–VI/C	34 (17 female, 17 male)	80.0 (56–96)	2 hours 45 minutes–17 hours 35 minutes

different regions and stages. The postmortem intervals between death and tissue processing were between 2 hours 15 minutes and 17 hours 35 minutes. An individual summary of cases, sex, age, postmortem delay, and diagnosis is shown in Table, Supplemental Digital Content 1 (http://links.lww.com/NEN/A705).

Whole-Transcript Expression Arrays

RNA samples from the cerebral cortex of APP/PS1 and WT littermates aged 3, 6, and 12 months were analyzed using the Affymetrix microarray platform and the GeneChip Mouse Gene 1.1 ST Array. This array analyzes gene expression patterns on a whole-genome scale on a single array, with probes covering several exons on target genes. Starting material was 200 ng of total RNA of each sample. Quality of isolated RNA was first measured with BioAnalyzer Assay (Agilent, Santa Clara, CA); RIN values were higher than 8. Sense single-stranded DNA suitable for labeling was generated from total RNA with the Ambion WT Expression Kit (Ambion, Carlsbad, CA) according to the manufacturer's instructions. Sense single-stranded DNA was fragmented, labeled, and hybridized to the arrays with the GeneChip WT Terminal Labeling and Hybridization Kit (Affymetrix, Santa Clara, CA). Chips were processed on an Affymetrix GeneTitan platform.

Microarray Data Normalization and Differential Expression Analysis

Preprocessing of raw data and statistical analyses were performed using Bioconductor packages in R programming environment (58). We read CEL files from Affymetrix arrays and corrected the background, and then summarized and normalized the data with the Robust Microarray Analysis method implemented in the Bioconductor Limma package (59). Furthermore, we estimated fold change and standard errors by fitting a linear model (using the lmFit function in Limma package) for each gene given the groups of arrays. Genes with empirical Bayes *t*-test p values of 0.05 were selected and corrected by calculating the false discovery rate $p < 0.05$ (''adjusted probability'').

Functional Enrichment Analysis

To evaluate which pathways or functional categories were enriched in APP/PS1 samples, we followed a similar strategy as previously described (60). Briefly, we performed Gene Set Enrichment Analysis using Limma package and hypergeometry-based tests using GOstats package (61). We used $p < 0.05$ as cutoff point to determine whether Gene Ontology (GO) terms or Kyoto Encyclopedia of Genes and Genomes (KEGG) pathways were significantly enriched.

The GeneSetTest function in Limma package tests whether a set of genes is enriched for differential expression. Its principle is the same as that of Gene Set Enrichment Analysis (62), but the statistical tests used are different. It is based on a set of probewise *t*-statistics arising for microarray analysis. We computed 3 different tests: i) upregulated genes with positive *t*-statistics; ii) downregulated genes with negative *t*-statistics; and iii) upregulated or downregulated genes as a whole. We used GOstats package to determine GO terms and KEGG pathways enriched in the subset of genes with differential

TABLE 2. TaqMan Probes Used to Study the Expression of Cytokines and Mediators of Immune Response in Mice

Symbol	Gene Name	TaqMan Sequences
Hprt	Hypoxanthine-guanine phosphoribosyltranferase	CAGCAGTGAGGACAAAACCGAGTTT
AARS	Alanyl-transfer RNA synthase	GGACTGATTATGGACAGGACTGAAA
Xpnpep1	X-Prolyl aminopeptidase (aminopeptidase P) 1	ACTACGCGCCAGTCCCTGAGACGAA
C1ql1	Complement component 1, q subcomponent 1	AACGGCCAGGTGCGGGCCAGTGCAA
C1qtnf7	C1q and tumor necrosis factor–related protein 7	AAAGGGCACTGCAGGTCTAAAAGGT
C3ar1	Complement component 3a receptor 1	GTGTGCTTGACTGAGCCATGGAGTC
C4b	Complement component 4b	GACATGAGCAAGGTCTTTGAAGTAA
Csf1r	Colony-stimulating factor 1 receptor	CTAAAAACTGCATCCACCGGGACGT
Csf3r	Colony-stimulating factor 1 receptor	GCTACTCCCCAGAAGTCTGGAGAGC
Tlr4	Toll-like receptor 4	CCCTGCATAGAGGTAGTTCCTAATA
Tlr7	Toll-like receptor 7	CCCTGCATAGAGGTAGTTCCTAATA
Ccl3	Chemokine (C-C motif) ligand 3	GTCTTCTCAGCGCCATATGGAGCTG
Ccl4	Chemokine (C-C motif) ligand 4	GTTCTCAGCACCAATGGGCTCTGAC
Ccl6	Chemokine (C-C motif) ligand 6	CCCAGGCTGGCCTCATACAAGAAAT
CxCl10	Chemokine (C-X-C motif) ligand 10	GACTCAAGGGATCCCTCTCGCAAGG
Il1b	Interleukin-1β	GACCCCAAAAGATGAAGGGCTGCTT
Il6	Interleukin-6	TGAGAAAAGAGTTGTGCAATGGCAA
Il6st	Interleukin-6 signal transducer	ACCCACTTGAGAGGACGCCTCCTGG
Tnfα	Tumor necrosis factor-α	GCCCACGTCGTAGCAAACCACCAAG
Tnfrsf1a	Tumor necrosis factor receptor superfamily member 1a	CTTGCAGCCACTGCAAGAAAAATGA
Il10	Interleukin-10	GAAGACTTTCTTTCAAACAAAGGAC
Il10ra	Interleukin-10 receptor α	TATCACGACGGAGCAGTATTTCACT
Il10rb	Interleukin-10 receptor β	CAGGCAATGACGAAATAACCCCTTC
Tgfβ1	Transforming growth factor-β1	CTGAACCAAGGAGACGGAATACAGG
Tgfβ2	Transforming growth factor-β2	TCGAGGCGAGATTTGCAGGTATTGA

expression in APP/PS1 versus WT groups at $p < 0.05$ (adjusted probability).

RNA Purification

Purification of RNA from mouse frontal cortex and human frontal cortex area 8, orbitofrontal cortex, and entorhinal cortex was carried out with RNeasy Lipid Tissue Mini Kit (Qiagen GmbH, Hilden, Germany) following the protocol provided by the manufacturer. Quality of isolated RNA was first measured with BioAnalyzer Assay (Agilent). RIN values in human cases are shown in Table, Supplemental Digital Content 1 (http://links.lww.com/NEN/A705). The concentration of each sample was obtained from A_{260} measurements with Nanodrop 1000 (Thermo Scientific, Wilmington, DE). RNA integrity was tested using the Agilent 2100 BioAnalyzer (Agilent Technologies, Palo Alto, CA).

Retrotranscription Reaction

Retrotranscription reaction was carried out using a High-Capacity cDNA Archive Kit (Applied Biosystems, Foster City, CA) following the protocol provided by the supplier. Parallel reactions for an RNA sample were run in the absence of MultiScribe Reverse Transcriptase to assess the degree of contaminating genomic DNA.

TaqMan PCR

TaqMan quantitative RT-PCR assays for each gene were performed in duplicate on complementary DNA samples in 384-well optical plates using an ABI Prism 7900 Sequence Detection System (Applied Biosystems). For every 10 μL of TaqMan reaction, 4.5 μL of complementary DNA was mixed with 0.5 μL of 20× TaqMan Gene Expression Assays and 5 μL of 2× TaqMan Universal PCR Master Mix (Applied Biosystems). Parallel assays for each sample were carried out using probes for hypoxanthine-guanine phosphoribosyltranferase, alanyl-transfer RNA synthase, X-prolyl aminopeptidase (aminopeptidase P) 1, and β-glucuronidase (β-Gus; only in human cases) for normalization (63, 64). Reactions were carried out using the following parameters: 50°C for 2 minutes, 95°C for 10 minutes, and 40 cycles of 95°C for 15 seconds and 60°C for 1 minute. Finally, all TaqMan PCR data were captured using Sequence Detection Software version 1.9 (Applied Biosystems). The identification numbers and names of all TaqMan probes (Applied Biosystems) used in the study of murine cortex are shown in Table 2, and those of probes used in the human study (Applied Biosystems) are shown in Table 3. Nearly the same mRNAs were analyzed in murine and human samples for comparative purposes between AD and the APP/PS1 model. The number of probes, including members of the complement system, colony-stimulating factor receptors, Toll-like receptors, pro-inflammatory cytokines, interleukin (IL) 6, members of the tumor necrosis factor (TNF) family, IL10 and its receptors, and transforming growth factor-β (TGFβ) family, is the largest analyzed to date.

Murine and human samples were analyzed with the double-delta cycle threshold ($\Delta\Delta C_T$) method. ΔC_T values represent normalized target gene levels with respect to internal control. $\Delta\Delta C_T$ values were calculated as the ΔC_T of each test sample minus the mean ΔC_T of calibrator samples (3-month-old WT mice or human controls) for each target gene. Fold change was determined using the equation $2^{(-\Delta\Delta C_T)}$.

Results in mice were analyzed with 2-way analysis of variance, followed by 1-way analysis of variance and Tukey post hoc or Student *t*-test. *T*-test was used to compare data in a

TABLE 3. TaqMan Probes Used to Study the Expression of Cytokines and Mediators of Immune Response in Human Brains

Symbol	Gene Name	TaqMan Sequences
HRPT	Hypoxanthine-guanine phosphoribosyltranferase	GGACTAATTATGGACAGGACTGAAC
AARS	Alanyl-transfer RNA synthase	GCAAAATTTGGGGCTGGATGACACC
XPNPEP1	X-Prolyl aminopeptidase (aminopeptidase P) 1	CAAAGAGTGCGACTGGCTCAACAAT
GUS-B	Beta-glucuronidase	GCTACTACTTGAAGATGGTGATCGC
C1QL1	Complement component 1, q subcomponent 1	CTGCAAGAATGGCCAGGTGCGGGCC
C1QTNF7	C1q and tumor necrosis factor–related protein 7	GGGAACTGCAGGTTTGAGAGGTAAG
C3AR1	Complement component 3a receptor 1	TCTCAGTTTTTTGAAGTTTAGCAAT
CSF1R	Colony-stimulating factor 1 receptor	CCAAAGAATATATACAGCATCATGC
CSF3R	Colony-stimulating factor 1 receptor	GCTGCTCCCCGGAAGTCTGGAGGAG
TLR4	Toll-like receptor 4	GGAGCCCTGCGTGGAGGTGGTTCCT
TLR7	Toll-like receptor 7	AGACTAAAAATGGTGTTTCCAATGT
IL8	Interleukin-8	GTGTGAAGGTGCAGTTTTGCCAAGG
IL1B	Interleukin-1β	CAGATGAAGTGCTCCTTCCAGGACC
IL6	Interleukin-6	TCAGCCCTGAGAAAGGAGACATGTA
IL6ST	Interleukin-6 signal transducer	CAAAGTTTGCTCAAGGAGAAATTGA
TNFα	Tumor necrosis factor-α	TGGCCCAGGCAGTCAGATCATCTTC
TNFRSF1A	Tumor necrosis factor receptor superfamily member 1a	CTCCTGTAGTAACTGTAAGAAAAGC
IL10	Interleukin-10	AATAAGCTCCAAGAGAAAGGCATCT
IL10RA	Interleukin-10 receptor α	CAGTGTCCTGCTCTTCAAGAAGCCC
IL10RB	Interleukin-10 receptor β	TCCACAGCACCTGAAAGAGTTTTTG
TGFβ1	Transforming growth factor-β1	AGTACAGCAAGGTCCTGGCCCTGTA
TGFβ2	Transforming growth factor-β2	GCACAGCAGGGTCCTGAGCTTATAT

given region and at a given Braak and Braak stage in sAD and their corresponding control groups. The significance level was set at $p < 0.05$ for all experiments.

Western Blot Analysis

Human frontal cortex area 8 and murine cerebral cortex samples were lysed in lysis buffer: 100 mmol/L Tris (pH 7), 100 mmol/L NaCl, 10 mmol/L ethylenediaminetetraacetic acid, 0.5% NP-40, and 0.5% sodium deoxycholate plus protease and phosphatase inhibitors (Roche Molecular Systems, Pleasanton, CA). After centrifugation at 14,000 × *g* for 20 minutes at 4°C (Ultracentrifuge Beckman with 70Ti rotor), supernatants were quantified for protein concentration (bicinchoninic acid assay; Pierce, Waltham, MA), mixed with sodium dodecyl sulfate (SDS)–polyacrylamide gel electrophoresis (PAGE) sample buffer, boiled, and subjected to 8%–15% SDS-PAGE. Gels were electrophoretically transferred onto nitrocellulose membranes (200 mA per membrane, 20 minutes). Nonspecific binding was blocked by incubation in 5% albumin in phosphate-buffered saline (PBS) containing 0.2% Tween for 1 hour at room temperature. After washing, the membranes were incubated at 4°C overnight with one of the following rabbit polyclonal antibodies in PBS containing 5% albumin and 0.2% Tween: anti-IL1β (diluted 1:1000; Abcam, Cambridge, United Kingdom), anti-IL10 (AP52181PU-N, diluted 1:250; Acris Antibodies, Herford, Germany), and anti-IL6 (diluted 1:1000; Abcam); anti–β-actin (A5316, diluted 1:30,000; Sigma-Aldrich, St. Louis, MO) was blotted for control of protein loading. Membranes were then incubated for 1 hour with the appropriate horseradish peroxidase–conjugated secondary antibody (1:1000; Dako, Glostrup, Denmark), and immune complexes were revealed by a chemiluminescence reagent (electrochemiluminescence; Amersham, GE Healthcare, Buckinghamshire, United Kingdom).

Densitometries were carried out with ImageJ software, and values were normalized using β-actin. Normalized values were expressed as fold change from values obtained in control samples. Statistical analysis between groups was performed with 1-way analysis of variance followed by Tukey test using the Statgraphics Statistical Analysis and Data Visualization Software version 5.1. Differences between groups were considered statistically significant at * $p < 0.05$, ** $p < 0.01$, *** $p < 0.001$.

Immunohistochemistry

Formalin-fixed paraffin-embedded tissue sections (4–5 μm thick) of human entorhinal cortex and frontal cortex area 8 were dewaxed and processed for ionized calcium-binding adapter molecule-1 (Iba1) immunohistochemistry. Paraformaldehyde-fixed cryoprotected sections (7 μm thick) of human entorhinal cortex and cerebral cortex (area 8) were obtained with a cryostat and processed free-floating for IL6, IL10, nuclear factor κB (NFκB) p65, and TNF immunohistochemistry. Samples were obtained from MA individuals and at the first (Stages I–II/0 of Braak and Braak classification) and advanced (Stages V–VI/C) stages of AD-related pathology. The sections were incubated in 2% hydrogen peroxide and 10% methanol for 30 minutes at room temperature, followed by 5% normal serum for 2 hours. Then the sections were incubated overnight with one of the primary antibodies. Antibodies to Iba1 (ab178680, diluted 1:250; Abcam) were used. We used rabbit polyclonal antibodies to IL6 (ab6672, diluted 1:100; Abcam), IL10 (AP52181PU-N, diluted 1:1000; Acris Antibodies), and NFκB-p65 (8242, diluted 1:1000; Cell Signaling, Danvers, MA), and mouse monoclonal antibodies to TNF (ab1793, diluted 1:10; Abcam). Peroxidase reaction was visualized with diaminobenzidine and H_2O_2. Control of immunostaining included omission of the primary antibody; no signal was obtained after incubation with only the secondary antibody.

Immunohistochemistry of Aβ Plaque Burden in AD

Fixed tissue samples were embedded in paraffin, and 4-μm-thick coronal sections were cut with a microtome. Consecutive dewaxed sections were incubated in 98% formic acid (3 minutes) and then treated with citrate buffer (20 minutes) to enhance antigenicity. Endogenous peroxidases were then blocked by incubation in 10% methanol–1% H_2O_2 solution (15 minutes). Sections were blocked with 3% normal horse serum solution and then incubated at 4°C overnight with primary antibodies to total Aβ (clone 6 F/3D, diluted 1:50; Dako), Aβ40 (diluted 1:100; Merck Millipore, Billerica, MA), or Aβ42 (diluted 1:50; Merck Millipore). Sections were subsequently rinsed and incubated with biotinylated secondary antibody (Dako), followed by EnVision + System peroxidase (Dako) and, finally, chromogen diaminobenzidine and H_2O_2. Sections were lightly counterstained with hematoxylin. After staining, the sections were dehydrated and coverslipped for observation under a Nikon Eclipse E800 microscope (40× objective; Nikon Imaging Inc, Tokyo, Japan). The cortical total Aβ burden was calculated as the percentage of the area of Aβ deposition in plaques with respect to the total area in 9 representative pictures taken from every region and stage. The ratios between Aβ42 and Aβ40 deposition were calculated by comparing specific staining with each antibody in consecutive sections. Beta-amyloid quantification was assessed using the Adobe Photoshop CS4 software (Adobe Systems Inc, San Jose, CA).

Concentrations of Aβ40 and Aβ42

Frozen samples of the entorhinal, orbitofrontal, and frontal cortices of sAD cases and corresponding controls were homogenized in Tris-buffered saline (TBS; 140 mmol/L NaCl, 3 mmol/L KCl, 25 mmol/L Tris-HCl [pH 7.4], and 5 mmol/L ethylenediaminetetraacetic acid) with a cocktail of protease inhibitors (Roche Molecular Systems) and ultracentrifuged at 100,000 × *g* for 1 hour at 4°C. The supernatant was the soluble fraction used for amyloid quantification, and the protein of this fraction was measured with bicinchoninic acid assay. Detection and measurement of Aβ40 and Aβ42 were carried out with enzyme-linked immunosorbent assay (ELISA) using the corresponding detection kits (Invitrogen, Camarillo, CA), following the instructions of the supplier. Levels of Aβ40 and Aβ42 were normalized to the total amount of protein from each individual sample.

Quantification of Membrane-Associated Aβ

Frozen samples of the entorhinal cortex, orbitofrontal cortex, and frontal cortex area 8 of sAD cases and MA individuals were homogenized in TBS with a cocktail of protease

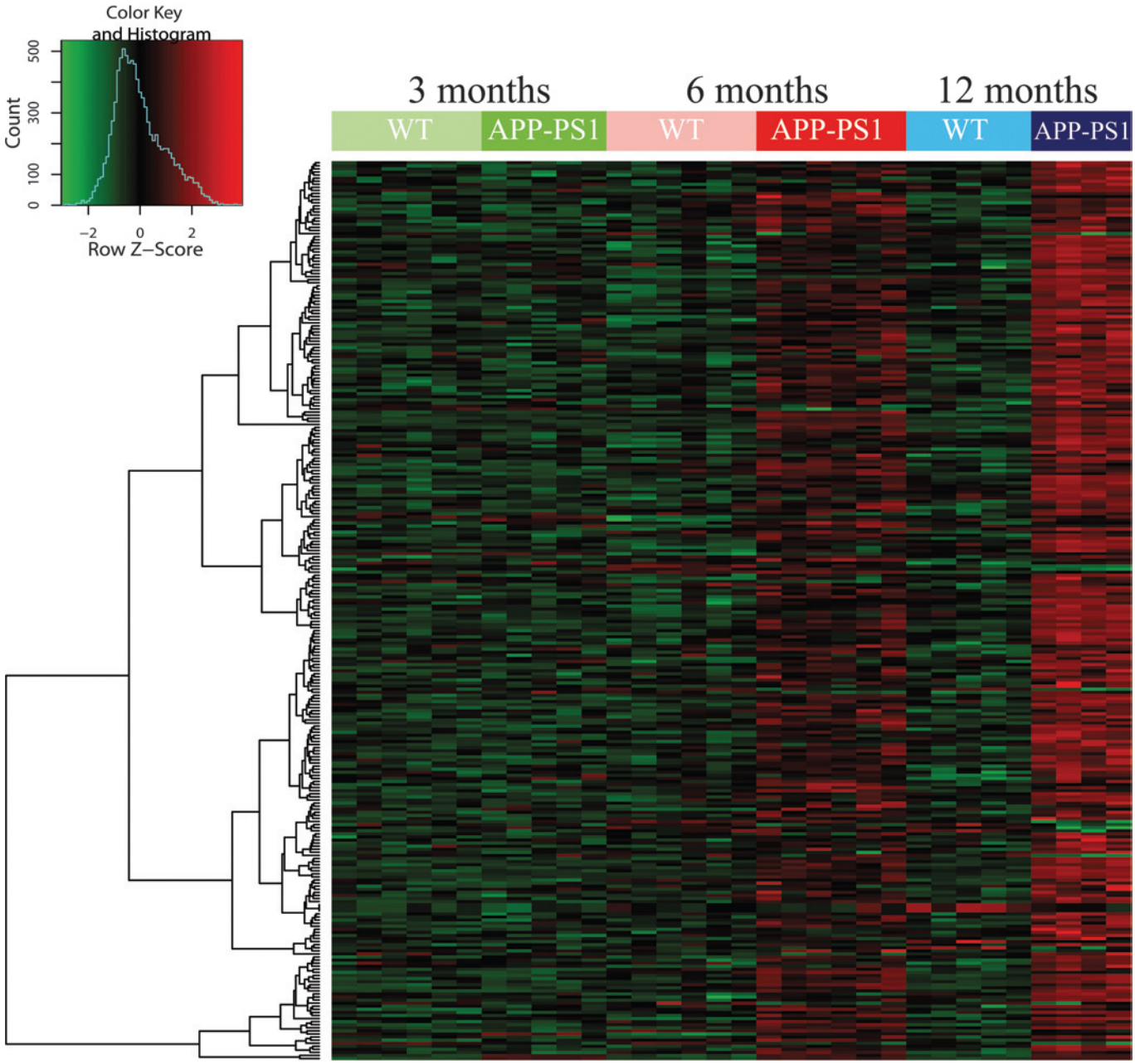

Fig 1 4/C

FIGURE 1. A hierarchical clustering heatmap of the expression intensities of significantly regulated transcripts (y axis) versus APP-PS1 and WT arrays (x axis). A clear separation is seen between APP/PS1 and WT mice at 6 and 12 months of age. We scaled the expression intensities on rows (probe sets/genes) to *Z* scores to make them weigh equally in the clustering. The colors of the heatmap are mapped linearly to the *Z* scores (low expression in green and high expression in red).

and phosphatase inhibitors (Roche Molecular Systems). Homogenates were centrifuged at 14,000 × *g* for 30 minutes at 4°C. The pellet was resuspended in 2% SDS and centrifuged at 14,000 × *g* for 30 minutes at 4°C. The supernatant was membrane-associated Aβ, and the protein of this fraction was measured with bicinchoninic acid assay. Proteins were separated in SDS-PAGE. Thirty-five micrograms of protein was loaded onto a precast NuPAGE 4%–12% Bis-Tris gel system (Invitrogen) with MES buffer (Invitrogen). The proteins were transferred to nitrocellulose membranes (200 mA per membrane for 90 minutes). Membranes were then boiled with PBS for 6 minutes, and nonspecific binding was blocked by incubation in 5% nonfat dry milk in TBS containing 0.2% Tween for 1 hour at room temperature. After washing, the membranes were incubated at 4°C overnight with the primary antibody to human Aβ protein, clone 4G8 (1:500; Covance, Princeton, NJ), in TBS containing 5% albumin and 0.2% Tween. Membranes were then incubated for 1 hour with the appropriate horseradish peroxidase–conjugated secondary antibody (1:2000; Dako), and immune complexes were visualized

AQ2 AQ5

TABLE 4. Common GO Terms for Molecular Function Enriched in APP/PS1 Mice at 6 and 12 Months of Age, Using Hypergeometric Distribution Function Statistical Analysis

			6 Months		12 Months	
GO ID	Term	Size	p Value	Count	p Value	Count
GO:0019864	IgG binding	5	$2.69E^{-09}$	4	$1.67E^{-07}$	4
GO:0005515	Protein binding	5,306	$1.31E^{-08}$	52	$4.31E^{-09}$	116
GO:0019865	Immunoglobulin binding	10	$1.11E^{-07}$	4	$6.66E^{-06}$	4
GO:0005126	Cytokine receptor binding	133	$2.90E^{-07}$	8	0.00048627	8
GO:0008009	Chemokine activity	32	$4.59E^{-07}$	5	0.00090088	4
GO:0019763	Immunoglobulin receptor activity	5	$1.13E^{-06}$	3	$2.46E^{-05}$	3
GO:0019770	IgG receptor activity	2	$2.37E^{-05}$	2	0.00018539	2

AQ2 with a chemiluminescence reagent (electrochemiluminescence; Amersham). Control of protein loading was checked by estimation of β-actin expression levels in the same membranes.

Dot Blot Assay

Frozen samples of the entorhinal cortex, orbitofrontal cortex, and frontal cortex area 8 of MA cases and in sAD Stages 0, A, B, and C were homogenized in TBS with a cocktail of protease inhibitors (Roche Molecular Systems) and ultracentrifuged at 100,000 × *g* for 1 hour at 4°C. Five micrograms of each soluble sample was applied to nitrocellulose membranes using a 48-well Dot Blot Manifold (Cleaver Scientific, Rugby, United Kingdom). The membranes were blocked with 10% nonfat milk in TBS containing 0.01% Tween 20 at room temperature for 1 hour. The membranes were washed 3 times, for 5 minutes each, with TBS containing 0.01% Tween 20 and incubated for 2 hours at room temperature with rabbit polyclonal anti-oligomer antibody A11 (AHB0052, diluted 1:1000; Invitrogen ThermoFisher, Carlsbad, CA). After washing, the membranes were incubated for 1 hour with the appropriate horseradish peroxidase–conjugated secondary antibody (1:2000; Dako), and immune complexes were visualized with a chemiluminescence reagent (electrochemiluminescence; Amersham). AQ2

RESULTS

Global Expression Profiles Identify mRNA Deregulation of Pathways Related to Inflammatory and Immune Responses in the Cerebral Cortex of APP/PS1 Mice

We analyzed APP/PS1 and WT samples from the cerebral cortex of mice at 3, 6, and 12 months of age. First, mouse RNA probes were hybridized to an Affymetrix Mouse Gene 1.1 ST Array including more than 28,000 well-annotated genes

TABLE 5. Common GO Terms for Biologic Function Enriched in APP/PS1 Mice at 6 and 12 Months of Age, Using Hypergeometric Distribution Function Statistical Analysis

			6 Months		12 Months	
GO ID Number	GO Term Name	Size	p Value	Count	p Value	Count
GO:0002376	Immune system process	831	$2.05E^{-28}$	39	$2.15E^{-45}$	80
GO:0006955	Immune response	448	$2.44E^{-17}$	23	$3.19E^{-36}$	55
GO:0050896	Response to stimulus	2,570	$6.29E^{-15}$	4	$9.86E^{-29}$	108
GO:0002682	Regulation of immune system	357	$1.07E^{-14}$	19	$6.99E^{-27}$	42
GO:0006954	Inflammatory response	281	$3.87E^{-14}$	17	$3.40E^{-18}$	30
GO:0006952	Defense response	502	$4.15E^{-14}$	21	$1.19E^{-25}$	47
GO:0050776	Regulation immune response	218	$2.15E^{-13}$	15	$5.73E^{-26}$	34
GO:0009611	Response to wounding	434	$3.56E^{-13}$	19	$1.05E^{-20}$	39
GO:0002684	Positive regulation of immune system process	235	$6.43E^{-13}$	15	$1.32E^{-22}$	32
GO:004221	Response chemical stimulus	1,094	$1.79E^{-12}$	27	$5.61E^{-14}$	50
GO:0001775	Cell activation	371	$3.46E^{-12}$	17	$3.58E^{-24}$	40
GO:0009605	Response to external stimulus	455	$8.69E^{-12}$	18	$4.38E^{-11}$	28
GO:0045321	Leukocyte activation	343	$1.22E^{-11}$	16	$2.08E^{-22}$	20
GO:0002274	Myeloid leukocyte activation	63	$2.37E^{-11}$	9	$2.57E^{-22}$	20
GO:0006950	Response to stress	1,334	$2.98E^{-11}$	28	$2.77E^{-20}$	66
GO:0048583	Regulation of response to stimulus	430	$3.56E^{-11}$	8	$2.10E^{-17}$	15
GO:0019882	Antigen processing and presentation	45	$5.08E^{-116}$	8	$2.10E^{-17}$	15
GO:0048002	Antigen processing and presentation of peptide antigen	28	$6.47E^{-11}$	7	$1.59E^{-17}$	13
GO:0016064	Immunoglobulin-mediated immune response	72	$8.20E^{-11}$	9	$5.05E^{-14}$	15

''Count,'' number of differentially expressed genes that are annotated at the GO term; ''p value,'' probability values for each GO term tested; ''Size,'' number of GeneChip Array genes that are annotated at GO.

with more than 770,000 distinct probes. We found differential gene expression between APP/PS1 and WT mice in statistical linear models (Fig. 1). Next, we analyzed the functional enrichment of metabolic and cell signaling pathways as annotated in KEGG and GO terms. Significant KEGG pathways were identified using Gene Set Enrichment Analysis and hypergeometric distribution function. At 3 months of age, we could only detect significant alteration in the expression of 2 genes (*App* and *Prnp*), whereas at 6 months and 12 months, we identified 113 and 332 deregulated genes, respectively, with an overlap of 88 genes. From among all deregulated genes, 150 different genes were related to inflammation-related pathways, belonging to both innate and adaptive immune responses (Tables 4, 5). Other deregulated pathways are not the subject of the present study. The different immune-related pathways were organized according to GO and KEGG terms as follows: intestinal immune network for IgA production (4672); hematopoietic cell lineage (4640); FcγR-mediated phagocytosis (4666); cytokine–cytokine receptor interaction (4060); Toll-like receptor signaling pathway (4620); leukocyte transendothelial migration (4670); natural killer cell–mediated cytotoxicity (4650); complement and coagulation cascades (4610); chemokine signaling pathway (4062); antigen processing and presentation (4612); and B-cell receptor signaling pathway (4662) (Fig. 2). Microarray data are available in the ArrayExpress database (www.ebi.ac.uk/arrayexpress) under accession number E-MTAB-2121.

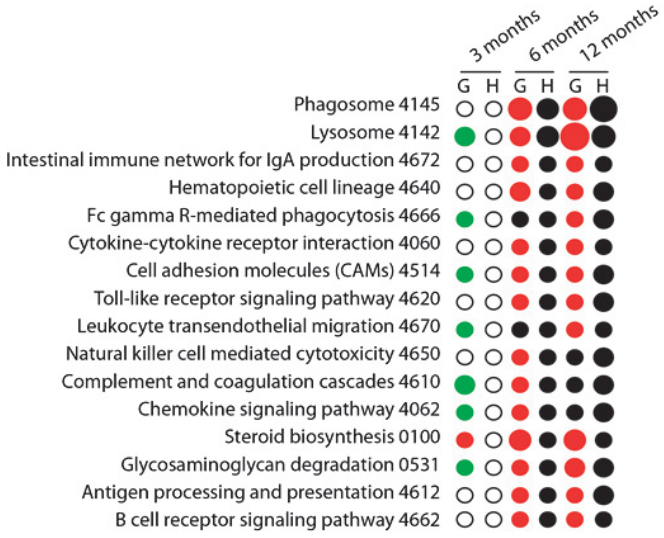

Fig 2 4/C

FIGURE 2. Regulated pathways in APP-PS1 mice at 6 and 12 months. Significant KEGG pathways were identified using Gene Set Enrichment Analysis (G) and hypergeometric distribution function (H). Only the statistically significant pathways using H are represented (6 and 12 months; no pathways were significantly different at 3 months). Red and green spots represent global upregulated and downregulated pathway expression, respectively, based on G test, for a probability of $p < 0.05$. Black spots represent modified regulated pathways based on H test, which detects changes but does not inform about their upward or downward direction, for a probability of $p < 0.05$. Spot size is within the scale of the probability value, with the lowest values for lysosome ($p = 2.94E^{-17}$ in G for 12 months of age) or phagosome ($p = 3.00E^{-14}$ and $p = 8.36E^{-09}$ in H for 6 and 12 months of age) when compared with controls.

mRNA Expression of Selected Inflammation-Related Genes in the Cerebral Cortex of WT and APP/PS1 Transgenic Mice With Age

We next carried out validation experiments using quantitative RT-PCR to measure expression levels of 22 inflammation-related genes, selected according to the most significant differential expression in transcriptomic experiments. A heatmap of the mRNA expression of selected cytokine-related genes involved in inflammatory response in WT and APP/PS1 mice aged 3, 12, and 20/22 months shows a clear separation between APP/PS1 and WT mice at 12 and 22 months of age (Fig. 3). Quantitative RT-PCR data at ages 3 and 12 months validated the microarray analysis, with all of them going up and down in the same way.

In control mice aged 3, 12, and 20/22 months, we detected increased expression of colony-stimulating factor receptor Csf1r, Toll-like receptor Tlr4, IL6 signal transducer (Il6st), and IL10 receptor 1β (il10rb); decreased Csf3r was also found in 12-month-old versus 3-month-old mice. However, there was a major shift in gene expression in control animals aged 20/22 months versus mice aged 12 months. Members of the complement system C1ql1, C3ar1, and C4b; colony-stimulating factor receptor Csf3r; Toll-like receptor Tlr7; chemokines Ccl3, Ccl4, and CxCl10; pro-inflammatory cytokines Il1β and Tnfα; and anti-inflammatory cytokines Il10 and Tgfβ1 significantly increased with age. In contrast, colony-stimulating factor receptor Csf1r, Toll-like receptor Tlr4, and il10rb were significantly decreased in the older group (Figure, Supplemental Digital Content 2, http://links.lww.com/NEN/A706).

Significant modifications in the mRNA expression of a large number of genes also occurred in APP/PS1 mice with age. Instead of 5 of 22 genes being differentially regulated in control 12-month-old versus aged 3-month-old mice, 15 genes were differentially regulated in APP/PS1 in the same lifetime, all of them dramatically upregulated and covering members of the complement system C1qtnf7 and C4b; colony-stimulating factor receptors Csf1r and Csf3r; Toll-like receptor Tlr4 and Tlr7; chemokines Ccl3, Ccl4, Ccl6, and CxCl10; pro-inflammatory cytokines Il6 and Il6st; and IL10 receptors 1α and 1β, and Tgfβ1. Eleven genes were differentially regulated in APP/PS1 mice aged 20/22 months versus APP/PS1 mice aged 3 months, whereas 7 of them were the same as those seen in APP/PS1 mice aged 12 months, although with distinct magnitudes of expression. Therefore, major modifications in gene expression occurred between months 12 and 20/22 in control mice, but between months 3 and 12 in APP/PS1 mice (Figure, Supplemental Digital Content 3, http://links.lww.com/NEN/A707).

When comparing mRNA expression levels in APP/PS1 mice aged 12 and 20/22 months, C3ar1, C4b, and Tlr7 mRNAs were significantly increased, but C1qtnf7, Csf1r, Tlr4, Ilst, Il10ra, and Il10rb were significantly decreased in APP/PS1 mice aged 20/22 months when compared with 12-month-old

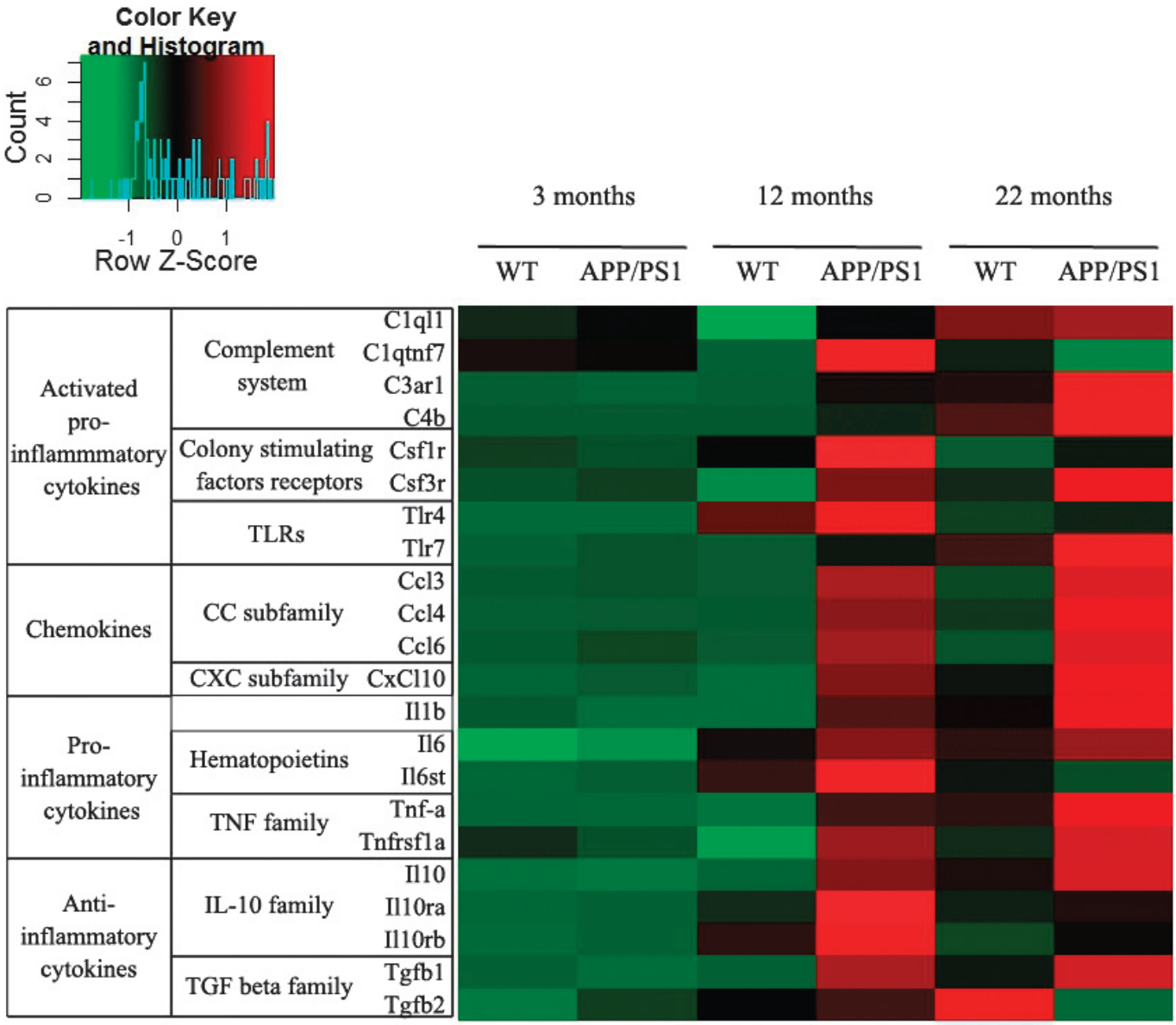

Fig 3 4/C

FIGURE 3. Heatmap of the mRNA expression of selected cytokine-related genes involved in inflammatory response in WT and APP/PS1 mice aged 3, 12, and 20/22 months. A clear separation is seen between APP/PS1 and WT mice at 12 and 20/22 months of age. Ccl3 and Ccl4 show marked mean (SE) fold differences of 32.4 (0.58) and 38.16 (7.26) and 33.37 (3.28) and 46.75 (7.69) at 12 and 20/22 months, respectively, in APP/PS1 versus WT mice at 3 months of age. We scaled the expression intensities on rows (probe sets/genes) to *Z* scores to make them weigh equally in the clustering. The colors of the heatmap are mapped linearly to the *Z* scores (low expression in green and high expression in red). AQ2

APP/PS1 mice (Figure, Supplemental Digital Content 3, http://links.lww.com/NEN/A707).

The mRNA expression of cytokines and mediators of immune response was compared between WT and APP/PS1 mice at different ages to discern whether the same genes were deregulated at early stages in transgenic mice when compared with WT. Increased mRNA expression of C3ar1, C4b, Csfr3, Tlr7, Ccl3, Ccl4, Ccl6, CxCl10, Il1b, Il6, Tnfα, Il10, Il10rb, and Tgfβ1 was found in WT mice at the age of 20/22 months. The expression of these genes was augmented in APP/PS1 transgenic mice at the age of 12 months. However, the expression of C1ql1, C1qtnf7, Il6st, Tnfrsf1a, and Il10ra was independent in WT and APP/PS1 mice at the ages of 20/22 and 12 months, respectively. Finally, there was at least a trend of decreased mRNA expression of Csf1r, Tlr4, Il10rb, and Il6st in WT and APP/PS1 transgenic mice at the age of 20/22 months.

Lastly, differences in gene expression values at peak points were compared in WT and APP/PS1 transgenic mice. Although several genes were increased in WT and APP/PS1 mice, mRNA expression in the latter was between 2 and 30 times higher at the age of 12 months, and between 2 and 10

TABLE 6. mRNA Expression of Selected Cytokine-Related Genes Involved in Inflammatory Response in WT and APP/PS1 Mice Aged 3, 12, and 20/22 (20) Months

			3 Months		12 Months		20 Months	
		Gene	WT	APP/PS1	WT	APP/PS1	WT	APP/PS1
Activated pro-inflammatory cytokines	Complement system	*C1ql1*	1.00 (0.03)	1.06 (0.03)	0.77 (0.06)	1.06 (0.10)	1.19 (0.12)*	1.23 (0.15)
		C1qtnf7	1.02 (0.09)	0.96 (0.06)	0.79 (0.10)	1.42 (0.14)†	0.91 (0.06)	0.73 (0.15)*
		C3ar1	1.00 (0.04)	0.82 (0.05)‡	1.01 (0.07)	4.39 (0.51)§	4.66 (0.29)¶,‖	10.48 (1.64)*,¶,**
		C4b	1.00 (0.05)	1.01 (0.07)	1.15 (0.10)	6.27 (0.38)§,¶	18.02 (3.41)¶,‖	35.40 (8.35)*,¶
	Colony-stimulating factor receptors	*Csf1r*	1.00 (0.03)	0.92 (0.05)	1.26 (0.08)†	2.42 (0.26)§,¶	0.87 (0.02)‖	1.17 (0.10)‡,‖
		Csf3r	1.00 (0.02)	1.12 (0.11)	0.65 (0.06)††	2.22 (0.22)§,††	1.25 (0.09)‖	2.85 (0.24)§,¶
	TLRs	*Tlr4*	1.00 (0.06)	1.00 (0.05)	2.37 (0.23)¶	3.38 (0.20)¶,**	1.29 (0.04)‖	1.50 (0.12)†,‖
		Tlr7	1.00 (0.03)	1.25 (0.08)‡	1.08 (0.05)	2.22 (0.20)§,¶	3.55 (0.31)¶,‖	6.52 (0.52)§,¶,‖
Chemokines	C-C subfamily	*Ccl3*	1.06 (0.16)	1.91 (0.29)‡	0.76 (0.07)	32.44 (5.58)§,††	2.93 (0.38)¶,‖	38.16 (7.26)§,¶
		Ccl4	1.06 (0.16)	1.37 (0.14)	1.94 (0.18)	33.37 (3.28)§,¶	6.50 (0.59)¶,‖	46.75 (7.69)§,¶
		Ccl6	1.05 (0.14)	1.69 (0.24)‡	0.89 (0.08)	9.90 (1.28)§,††	1.31 (0.15)‡‡	11.81 (2.07)§,¶
	C-X-C subfamily	*CxCl10*	1.10 (0.22)	1.34 (0.52)	0.95 (0.13)	6.03 (0.42)†,§	3.06 (0.47)¶,‖	8.26 (1.80)¶,**
Pro-inflammatory cytokines		*Il1b*	1.05 (0.13)	0.90 (0.14)	0.89 (0.09)	2.27 (0.46)**	1.83 (0.24)‖,††	3.34 (0.58)‡,††
	Hematopoietins	*Il6*	1.05 (0.12)	1.15 (0.10)	1.60 (0.09)	1.86 (0.22)†	1.66 (0.28)†	1.90 (0.22)†
		Il6st	1.00 (0.03)	1.03 (0.03)	1.52 (0.12)††	2.15 (0.18)¶	1.27 (0.03)	1.09 (0.12)‖
	TNFα family	*Tnf*	1.04 (0.12)	1.01 (0.19)	0.89 (0.10)	2.65 (0.42)§	2.51 (0.28)¶,‖	4.23 (0.68)‡,¶
		Tnfrsf1a	1.00 (0.04)	0.94 (0.02)	0.82 (0.11)	1.29 (0.16)‡	1.00 (0.05)	1.37 (0.10)§
Anti-inflammatory cytokines	IL10 family	*Il10*	1.01 (0.07)	0.96 (0.13)	1.15 (0.11)	3.27 (0.43)§	2.43 (0.45)*,††	3.97 (0.92)†
		Il10ra	1.00 (0.03)	1.02 (0.06)	1.24 (0.14)	2.43 (0.36)¶,**	1.29 (0.03)	1.55 (0.14)‡‡
		Il10rb	1.00 (0.02)	1.06 (0.07)	2.09 (0.18)¶	3.48 (0.35)¶,**	1.26 (0.04)‖	1.69 (0.19)‖
	TGFβ family	*Tgfβ1*	1.00 (0.03)	0.95 (0.06)	1.00 (0.06)	2.21 (0.26)§,¶	1.36 (0.03)¶,‖	2.36 (0.15)§,¶
		Tgfβ2	1.00 (0.04)	1.07 (0.05)	1.14 (0.06)	1.21 (0.08)	1.41 (0.10)	1.02 (0.17)

Data are presented as mean (SE).
* $p < 0.01$, APP/PS1 or WT mice aged 20/22 months compared with corresponding APP/PS1 or WT mice aged 12 months (Tukey post hoc test).
† $p < 0.05$, APP/PS1 mice aged 3 months compared with APP/PS1 mice aged 12 and 20/22 months (Tukey post hoc test).
‡ $p < 0.05$, APP/PS1 mice compared with age-matched WT animals (Student *t*-test).
§ $p < 0.001$, APP/PS1 mice compared with age-matched WT animals (Student *t*-test).
¶ $p < 0.001$, APP/PS1 mice aged 3 months compared with APP/PS1 mice aged 12 and 20/22 months (Tukey post hoc test).
‖ $p < 0.001$, APP/PS1 or WT mice aged 20/22 months compared with corresponding APP/PS1 or WT mice aged 12 months (Tukey post hoc test).
** $p < 0.01$, APP/PS1 mice compared with age-matched WT animals (Student *t*-test).
†† $p < 0.01$, APP/PS1 mice aged 3 months compared with APP/PS1 mice aged 12 and 20/22 months (Tukey post hoc test).
‡‡

AQ7 AQ8

times higher at the age of 20/22 months. This phenomenon was clearly illustrated for chemokines and members of the complement system. A detailed summary of quantitative data is shown in Table 6. T6

mRNA Expression of Inflammation-Related Genes in Human Brain Aging and With sAD Progression and Its Relationship With Braak and Braak NFT Staging

To compare responses in regions with variable vulnerability to sAD and with progressive involvement during the neurodegenerative process, we carried out an analysis of inflammation-related genes in human brain samples from the entorhinal cortex, orbitofrontal cortex, and frontal cortex area 8. Neurofibrillary tangles were present in the entorhinal cortex at Stages I–II, did not appear or appeared only in very small numbers in the frontal cortex until Stage IV, and massively increased at Stages V and VI as defined by Braak and Braak classification.

In the entorhinal cortex, C3AR1, CSF3R, TLR7, IL1β, IL6, and IL10 mRNAs were increased at Braak and Braak Stages I–II/0(A) versus MA cases. Later on, C1QTNF7, C3AR1, TLR4, TLR7, and IL8 significantly increased with disease progression. However, IL1β, IL6, and IL10 were reduced at Braak and Braak Stages III–IV/A–B and V–VI/C when compared with cases at Braak and Braak Stages I–II/0(A) (Fig. 4). F4

In the orbitofrontal cortex, C3AR1, TLR7, IL1β, and IL6 mRNAs were also significantly increased at Braak and Braak Stages I–II/0(A) versus MA individuals. In addition, IL10, IL8, and C1QTNF7 mRNAs were upregulated at Braak and Braak Stages I–II/0(A). C3AR1, CSF1R, TLR7, IL10RA, TGFβ1, and TGFβ2 mRNA expression increased with disease progression. However, C1QTNF7, C3AR1, CSF1R, TLR7, IL8, IL1β, and IL6 mRNA expression decreased at Stages V–VI/C when compared with earlier Braak and Braak

F5 stages (Fig. 5). C1QL1, IL10RB, TNFα, and TNFRSF1A mRNAs were not modified in any region in cases with AD-related pathology versus MA cases.

In frontal cortex area 8, there was a significant increase in the mRNA expression of selected cytokines and mediators of immune response when comparing MA cases with cases with AD-related pathology at Stages I–II/0(A). Significant increases in mRNA expression levels of C3AR1, CSF1R, CSF3R, IL6, IL6ST, TGFβ1, and IL10RA were seen in AD cases at Stages I–II/0(A) of Braak and Braak classification when compared with MA individuals. Interestingly, although mRNA expression of all these mediators was increased at AD Stages III–IV/A–B and V–VI/C of Braak and Braak classification with respect to MA individuals and TGFβ2 significantly increased at Stages V–VI/C, there was a reduction in IL6, IL1, and CSF1R mRNAs with disease progression when compared with Stages I–II/0–A. Expression levels of IL10, IL10RB, IL8, TNFα, TNFRSF1A, C1QL1, C1QTNF7, and TLR3 mRNAs were not modified with age or disease pro-
F6 gression (Fig. 6).

mRNA Expression of Inflammation-Related Genes in Human Brain Aging and With sAD Progression and Its Relationship With Aβ Braak and Braak Plaque Staging

Messenger RNA expression of selected cytokines and mediators of immune response was also investigated at different stages of Aβ plaques according to Braak and
AQ2 Braak Stages 0–C. As shown in Tables, Supplemental Digital Content 1 (http://links.lww.com/NEN/A705), Supplemental Digital Content 4 (http://links.lww.com/NEN/A708), and Supplemental Digital Content 5 (http://links.lww.com/NEN/A709), modifications in gene expression occurred in the orbitofrontal cortex, entorhinal cortex, and frontal cortex area 8, albeit with regional variations, in 4 individuals with sAD Stage 0 (AD I–II of NFT pathology following Braak and Braak classification) versus MA individuals with no AD-related pathology. Gene regulation increased with plaque burden with disease progression, but again decreased in more advanced stages of the neurodegenerative process (Supplemental Digital Content 4, http://links.lww.com/NEN/A708; Supplemental Digital Content 5, http://links.lww.com/NEN/A709; and Supplemental Digital Content 6, http://links.lww.com/NEN/A710).

Protein Expression of Selected Cytokines in WT and APP/PS1 Transgenic Mice on Western Blot Analysis

Western blot analysis of IL1β revealed increased a significant increase in protein expression in WT mice aged 20/22 months versus younger mice, and a significant increase in APP/PS1 mice at the age of 12 and 20/22 months when compared with younger animals. Thus, protein levels paralleled mRNA expression values in WT and APP/PS1 mice at different ages. Significantly increased IL6 expression levels were found in WT animals aged 20/22 months and APP/PS1 mice aged 12 months when compared with expression levels at corresponding younger ages. A trend without statistical significance was also observed in APP/PS1 mice aged 20/22 months. Finally, a significant increase in the expression levels of IL10 was found in APP/PS1 mice compared with younger transgenic mice, thus paralleling mRNA observations. However, no apparent differences in the expression of IL10 was seen in WT animals aged 20/22 months (Fig. 7A). F7

Protein Expression of Selected Cytokines in Human Frontal Cortex Area 8 on Western Blot Analysis

Expression levels of IL1β were significantly increased in sAD Stages I–II/0(A) and III–IV/A–B when compared with younger individuals. A trend with no statistical significance was also observed in AD Stages V–VI/C. Expression levels of IL6 were significantly increased in all stages of sAD when compared with younger individuals, thus matching mRNA expression levels. In contrast to mRNA observations, a significant increase in IL10 protein expression was observed in sAD Stages V–VI/C when compared with the other groups (Fig. 7B).

Immunohistochemistry of Microglia and Selected Cytokines in Frontal Cortex Area 8 and Entorhinal Cortex in Middle Age and at the First and Advanced Stages of sAD

Ionized calcium-binding adapter molecule-1 immunohistochemistry revealed an increase in the number and size of microglia, together with predominance of ramified microglia, in sAD cases at Stages I–II/0(A) when compared with MA individuals. In addition to ramified microglia, many hypertrophic and round (amoeboid) microglia appeared at later stages (Figs. 8A–C). These observations are in line with previous studies F8 showing modifications in the morphology of microglia with aging and at the first stages of AD-related pathology (50, 51).

Localization of selected cytokines and mediators was also examined in the entorhinal cortex and frontal cortex area 8 in samples from MA individuals and at the first and advanced stages of sAD-related pathology. Immunohistochemistry showed expression of IL6, IL10, TNFα, and NFκB-p65 in microglial cells in MA and sAD cases (Figs. 8D–O). Similar profiles were seen in the frontal and entorhinal cortices. The pattern of IL6, IL10, TNFα, and NFκB-p65 immunostaining matched that of Iba1 immunohistochemistry. However, suboptimal immunostaining, together with individual variations, did not permit further quantification of cytokine expression in histologic sections.

Aβ Plaque Burden in the Entorhinal Cortex, Orbitofrontal Cortex, and Frontal Cortex Area 8 With Age and sAD Progression

Total Aβ plaque burden was assessed in the entorhinal cortex, orbitofrontal cortex, and frontal cortex area 8 by densitometric quantification of Aβ plaques, including diffuse and senile plaques, in sections processed for Aβ immunohistochemistry. Beta-amyloid burden was quantified in MA and sAD cases at Stages 0–C of Braak and Braak classification. By definition, no Aβ deposits were found in any of these regions in MA individuals and in cases with sAD-related

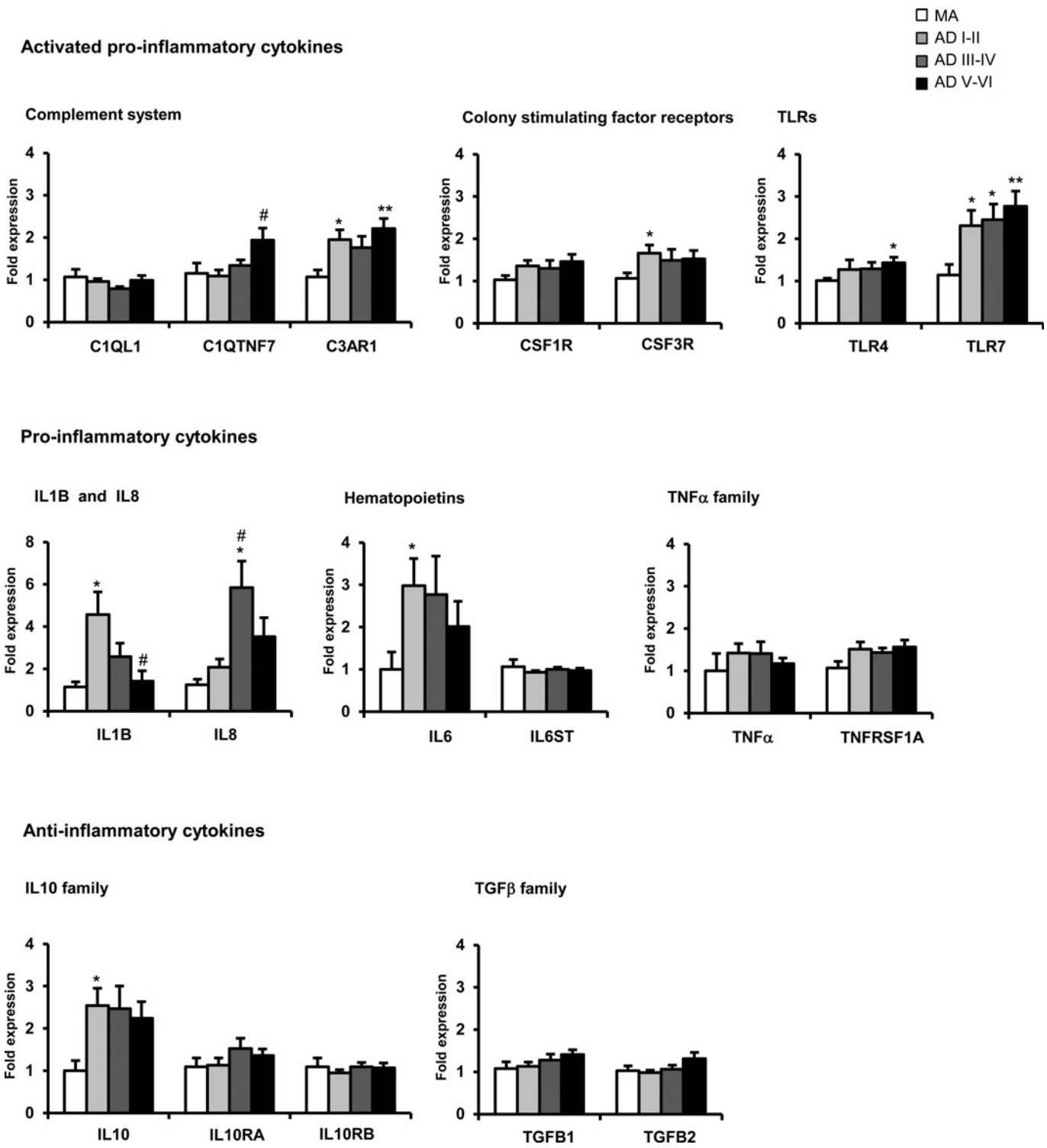

FIGURE 4. Messenger RNA expression of selected cytokines and mediators of immune response in the entorhinal cortex in MA individuals with no AD-related pathology and sAD cases: AD I–II, sAD I–II/0(A); AD II–IV, sAD III–IV/A–B; AD V–VI, sAD V–VI/B–C. C3AR1, CSF3R, TLR7, IL1β, IL6, and IL10 mRNAs are increased in the entorhinal cortex at Braak and Braak Stages I–II/0(A) when compared with MA cases. C1QTNF7, C3AR1, TLR4, TLR7, and IL8 significantly increase with disease progression. However, IL1β, IL6, and IL10 are reduced at Braak and Braak Stages III–IV/A–B and V–VI/C when compared with cases at Braak and Braak Stages I–II/0(A). Data are presented as mean (SE). * $p < 0.05$ and ** $p < 0.01$, differences in sAD at different stages versus MA cases. # $p < 0.05$, differences between sAD III–IV/A–B or sAD V–VI/C and sAD I–II/0(A).

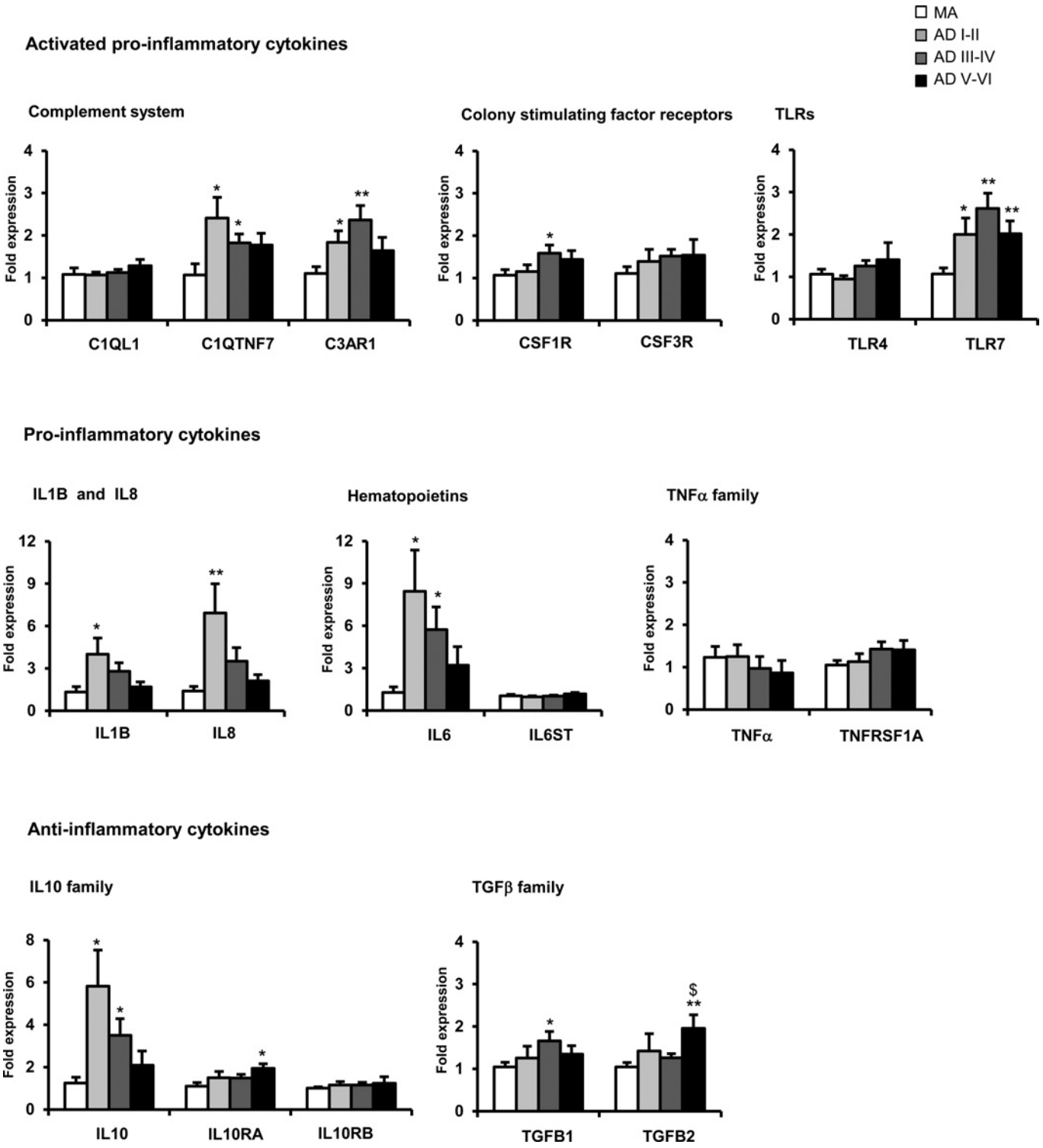

FIGURE 5. Messenger RNA expression of selected cytokines and mediators of immune response in the orbitofrontal cortex in MA individuals with no sAD-related pathology and AD cases: AD I–II, sAD I–II/0(A); AD II–IV, sAD III–IV/A–B; AD V–VI, sAD V–VI/B–C. C3AR1, TLR7, IL1β, and IL6 mRNAs are significantly increased in the orbitofrontal cortex at Stages I–II/0(A) when compared with MA individuals. IL10, IL8, and C1QTNF7 mRNAs are upregulated at Stages I–II/0(A). C3AR1, CSF1R, TLR7, IL10RA, TGFβ1, and TGFβ2 mRNA expression increases with disease progression. However, C1QTNF7, C3AR1, CSF1R, TLR7, IL8, IL1β, and IL6 mRNA expression decreases at Stages V–VI/C when compared with earlier stages. Data represent mean (SE). * $p < 0.05$ and ** $p < 0.01$, significant differences in AD at different stages versus MA cases. $^{\$}$ $p < 0.05$, differences between sAD V–VI/C and sAD III–IV/A–B.

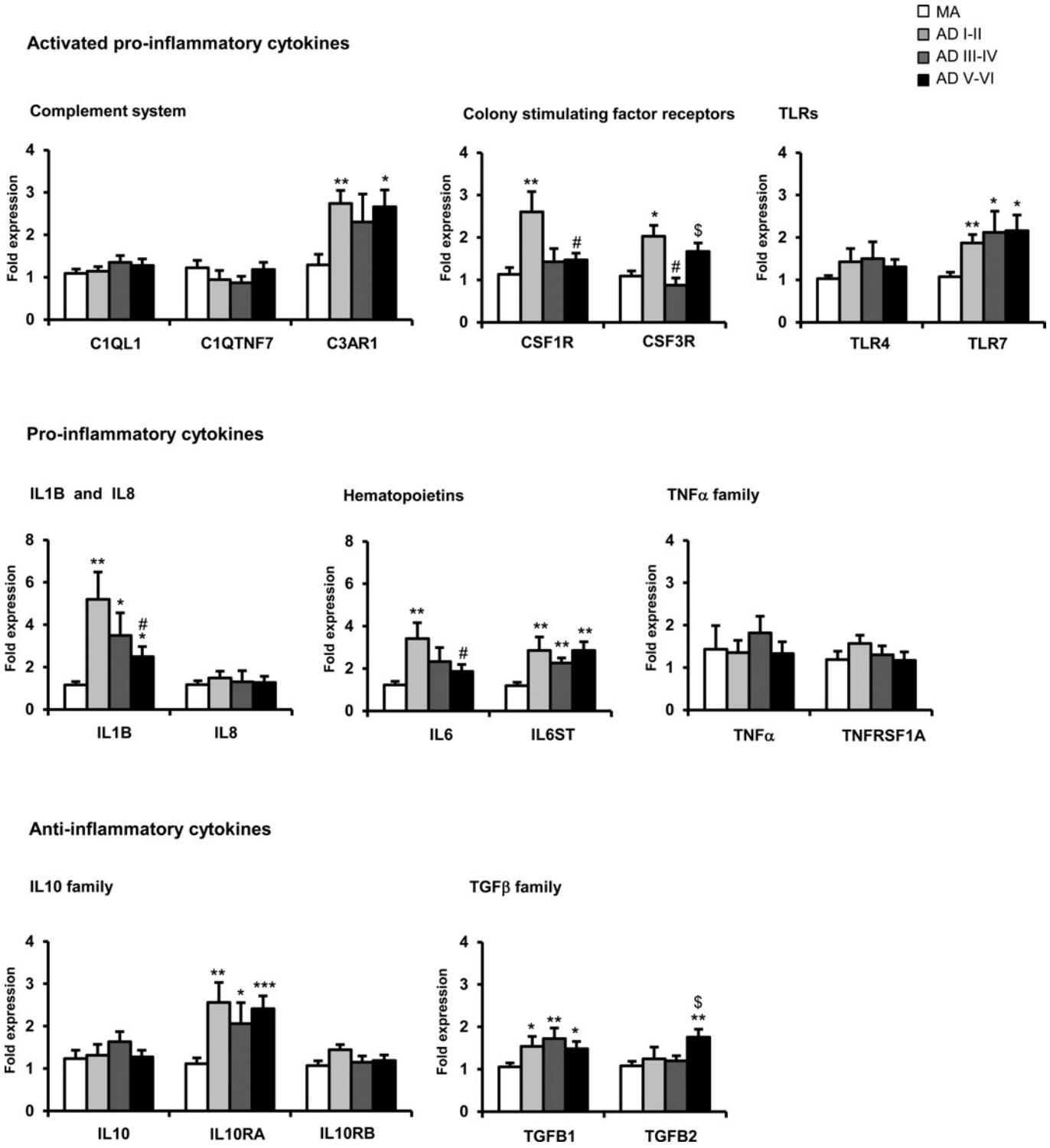

FIGURE 6. Messenger RNA expression of selected cytokines and mediators of immune response in frontal cortex area 8 in MA individuals with no sAD-related pathology and AD samples: AD I–II, sAD I–II/0(A); AD II–IV, sAD III–IV/A–B; AD V–VI, sAD V–VI/C. C3AR1, CSF1R, CSF3R, IL6, IL6ST, TGFβ1, and IL10RA are increased at Stages I–II/0(A) versus MA individuals. Messenger RNA expression of all these mediators is increased at AD Stages III–IV/A–B and V–VI/C with respect to MA individuals, and TGFβ2 significantly increases at Stages V–VI/C. However, IL6, IL1, and CSF1R mRNAs are reduced at advanced stages of AD when compared with Stages I–II/0–A. Data are presented as mean (SE). * $p < 0.05$, ** $p < 0.01$, *** $p < 0.001$, significant differences in sAD at different stages versus MA cases. # $p < 0.05$, differences between sAD III–IV/A–B or sAD V–VI/C and sAD I–II/0(A). $ $p < 0.05$, sAD V–VI/C versus sAD III–IV/A–B.

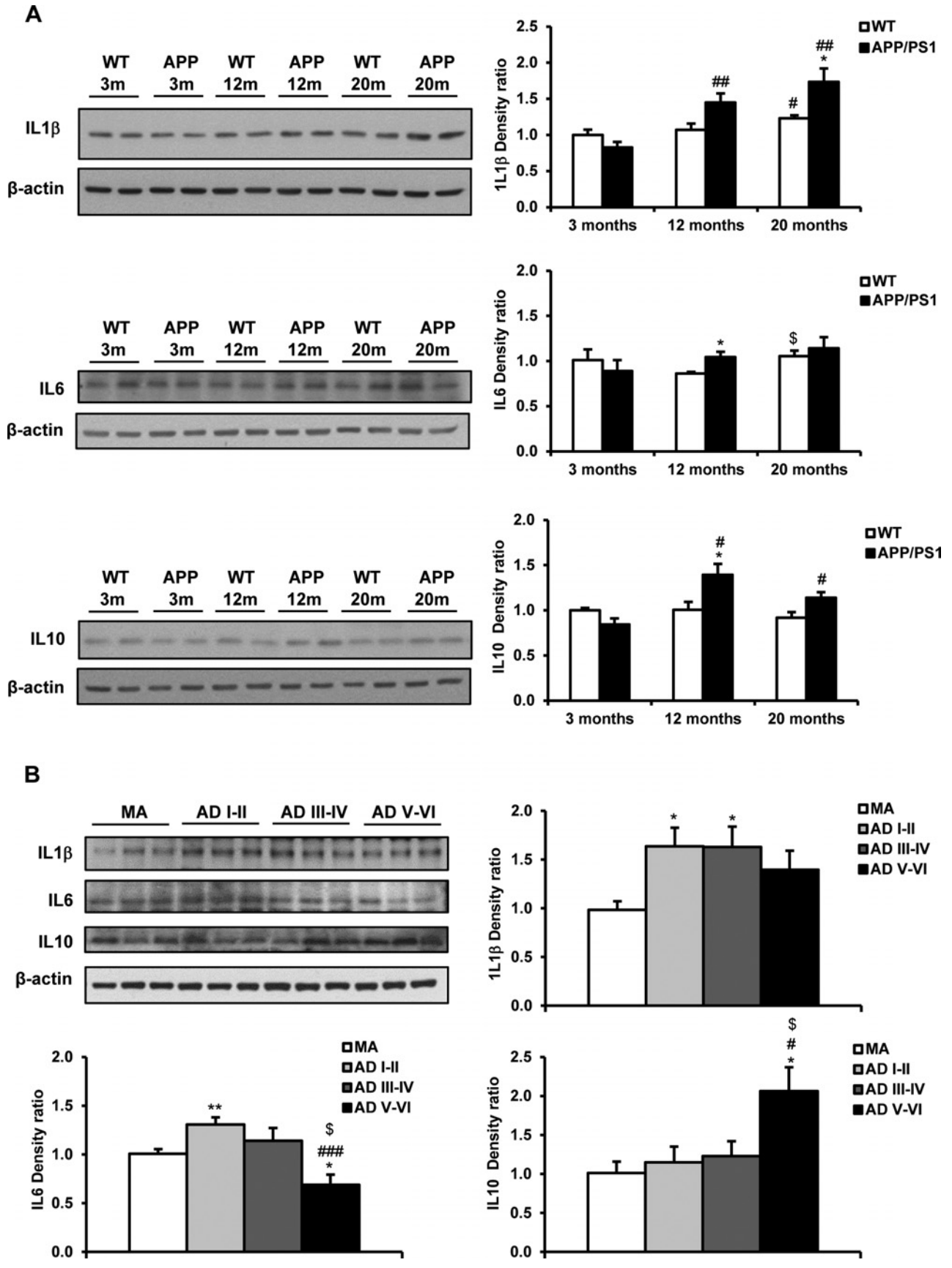

pathology at Stage 0 of Braak and Braak classification (most of those affected were at Stages I–II; 16 cases were at Stage 0 whereas 8 cases were at Stage A). The percentage of area occupied by Aβ deposits increased with stage progression (Fig. 9A). The composition of plaques differed with disease progression, with the amount of Aβ42 higher than that of Aβ40, as expected. Diffuse plaques were practically composed of Aβ42, whereas neuritic plaques were composed of Aβ42 and Aβ40. Because diffuse plaques predominated at early plaque stages, densitometry analysis of ratios between Aβ42 and Aβ40 varied from 25 to 35 at early stages to 10–20 at Stage C in the different cortical regions.

Concentrations of Aβ (Aβ40 and Aβ42) in the Entorhinal Cortex, Orbitofrontal Cortex, and Frontal Cortex Area 8 With Age and sAD Progression on ELISA

A significant increase in the levels of Aβ40 and Aβ42 in the orbitofrontal cortex was found at Stages I–II/0(A) of Braak and Braak classification when compared with MA individuals. Levels of Aβ40 and Aβ42 were higher at Stages V–VI/C (Fig. 9B). In contrast, a significant increase in Aβ40 and Aβ42 levels in the entorhinal cortex was not identified until Stages V–VI/C of Braak and Braak classification. No significant differences in the levels of Aβ40 and Aβ42 in the frontal cortex were seen in AD at Stages I–II/0(A) when compared with MA individuals. However, a significant increase in Aβ40 and Aβ42 occurred at Stages III–IV/A–B, which was augmented with disease progression at Stages V–VI/C (Fig. 9B).

To assess the relationship of Aβ concentrations and Braak and Braak stages of plaque burden, we determined Aβ40 and Aβ42 levels in middle age and at sAD Stages 0–C. Very low levels of Aβ40 and Aβ42 were detected in all regions in middle age and at Stage 0. Expression levels of Aβ40 and Aβ42 increased in all regions in sAD brains with stage progression (Fig. 9B). In contrast to that seen in plaques, Aβ42-to-Aβ40 ratios were between 0.4 and 0.8 in the entorhinal cortex, orbitofrontal cortex, and frontal cortex in MA and sAD cases, except for a ratio of 1 in frontal cortex area 8 at Stages V–VI/C of Braak and Braak classification.

Membrane-Associated Aβ Levels

Membrane-associated Aβ was detected in membrane-enriched fractions (which also contain non–membrane-associated proteins) blotted with anti–Aβ17–24 antibody. Control samples in all regions showed no detectable Aβ17–24 in membrane-enriched fractions. Membrane-associated Aβ was not detected in middle age and at sAD Stage 0 of Braak and Braak classification in any region. Membrane-associated Aβ17–24 was detected in low amounts only in about half of Stage A cases analyzed, but consistent levels of Aβ17–24 were found in all cases of sAD Stages B and C in the 3 regions examined (Fig. 9C).

Soluble Oligomers in the Human Entorhinal Cortex, Orbitofrontal Cortex, and Frontal Cortex, and in Murine Cerebral Cortex

Dot blots with the polyclonal anti-oligomer antibody A11 revealed a significant increase in the levels of soluble oligomers in the entorhinal cortex and frontal cortex, and a trend of increase without significance in the orbitofrontal cortex at Stage 0 of cases with sAD-related pathology versus MA individuals (Fig. 10). Values were also higher in the entorhinal cortex and frontal cortex area 8 at more advanced stages of AD, but they were only significant in the frontal cortex (Fig. 10). Interestingly, a significant increase in the expression levels of soluble oligomers was also observed in the cerebral cortex of WT mice at the age of 20/22 months when compared with mice aged 3 and 12 months (Fig. 10).

DISCUSSION

Gene Regulation and Expression of Cytokines and Mediators of Immune Response in sAD and APP/PS1 Transgenic Mice

Increased expression of cytokines and mediators of immune response at advanced stages of sAD and in related AD transgenic mice models is well established (14, 23–41). The present study demonstrates that inflammation-related responses are region- and stage-dependent during sAD progression when comparing the entorhinal cortex, orbitofrontal cortex, and frontal cortex area 8 at different stages of sAD. Moreover, our present analyses carried out in humans and mice permit a side-by-side comparisons and identification of commonalities and differences in transcriptomes in relation to species and stage of sAD progression.

Altered Gene Regulation of Cytokines and Mediators of Immune Response Is an Ordinary Phenomenon in Brain Aging in Humans and Mice

Aging is associated with changes in the immune system and increased production and release of inflammatory molecules by different organs and tissues, including adipose tissue and the cardiovascular system (mainly linked to arteriosclerosis); increased levels of circulating cytokines and mediators of the immune system characterize a process that has been named ''inflammatory aging'' (65, 66). The CNS is not an exception to this process, as innate immune cells in the brain

FIGURE 7. Western blot analysis of IL1β, IL6, and IL10 in murine and human cases. **(A)** Protein expression of cytokines in WT and APP/PS1 mice aged 3, 12, and 20/22 (20) months. * $p < 0.05$, APP/PS1 compared with age-matched WT animals (Student *t*-test). # $p < 0.05$, ## $p < 0.01$, WT or APP/PS1 mice aged 12 and 20/22 months versus corresponding WT or APP/PS1 mice aged 3 months (Student *t*-test). $ $p < 0.05$, WT aged 20/22 months versus WT aged 12 months (Student *t*-test). Beta-actin is used as control for protein loading. **(B)** Protein expression of cytokines in frontal cortex area 8 in MA cases and patients with sAD at different stages of Braak and Braak classification. * $p < 0.05$, ** $p < 0.01$, sAD versus MA cases. # $p < 0.05$, ### $p < 0.001$, sAD V–VI/C (AD V–VI) or III–IV/A–B (III–IV) versus I–II/0(A) (AD I–II). $ $p < 0.05$, sAD V–VI/C versus sAD III–IV/A–B. Beta-actin is used as control for protein loading.

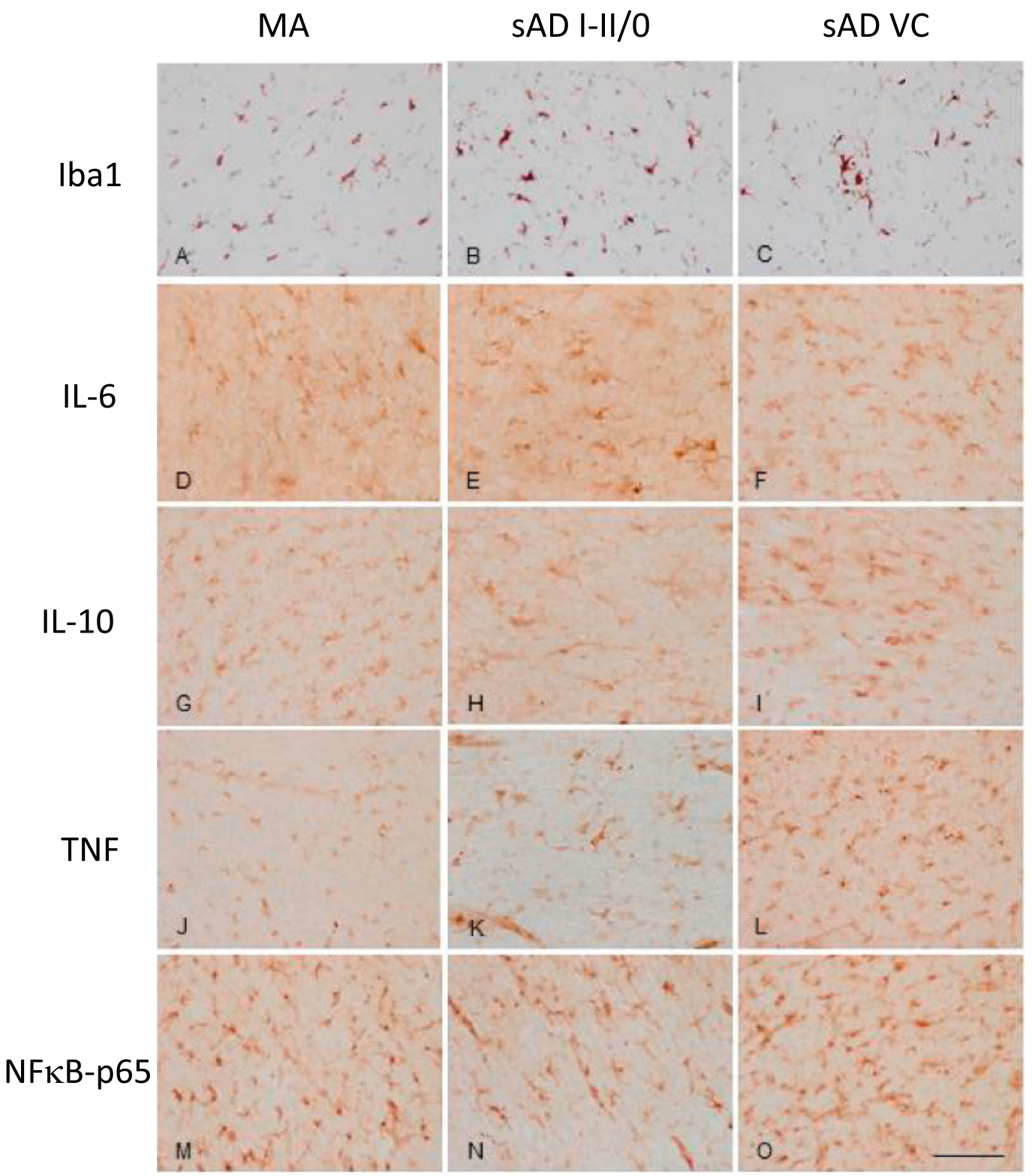

Fig 8 4/C

FIGURE 8. Microglial immunohistochemistry in frontal cortex area 8 in MA individuals **(A, D, G, J, M)** and cases with sAD-related pathology at Stages I–II/0 **(B, E, H, K, N)** and sAD Stage VC **(C, F, I, L, O)**. **(A–C)** Ionized calcium-binding adapter molecule-1; **(D–F)** IL6; **(G–I)** IL10; **(J–L)** TNF; **(M–O)** NFκB-p65. There is a major shift at the first stages of AD-related pathology, in which microglial cells appear ramified. **(A–C)** Formalin-fixed paraffin-embedded sections 5 μm thick; **(D–O)** paraformaldehyde-fixed cryoprotected tissue (7-μm-thick cryostat section) processed free-floating. Peroxidase reaction visualized with diaminobenzidine and H_2O_2 (**D–O**; without hematoxylin counterstaining). Scale bar = 25 μm.

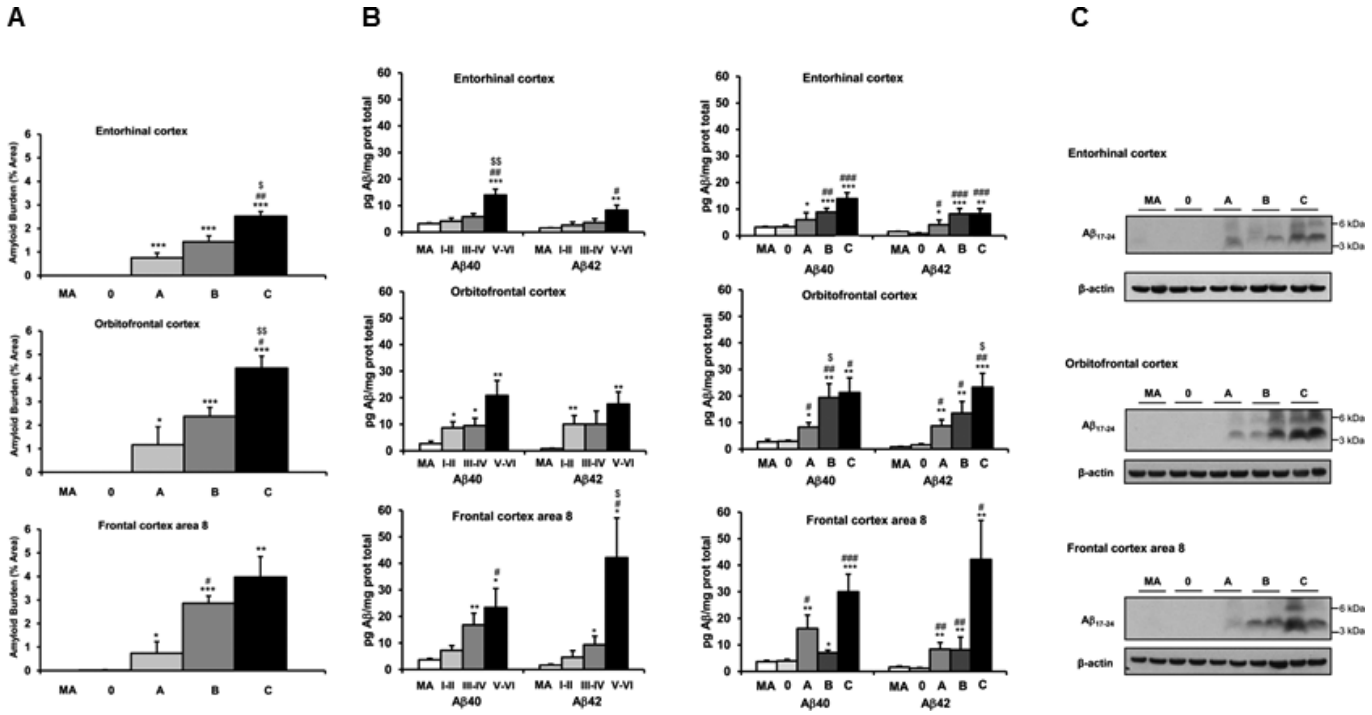

FIGURE 9. (A) Beta-amyloid plaque burden in MA individuals with no sAD-related pathology and cases with sAD-related pathology at Stages 0, A, B, and C. Values represent the percentage of the total cortical area occupied by Aβ plaques (either diffuse or neuritic plaques) in the entorhinal cortex, orbitofrontal cortex, and frontal cortex area 8. Data are presented as mean (SE). * $p < 0.05$, ** $p < 0.01$, *** $p < 0.001$, sAD at different Braak and Braak stages versus middle age. $^{\#}$ $p < 0.05$, differences between Stage B and Stage A. $^{\$,*}$ $p < 0.05$, ** $p < 0.01$, differences between Stage C and Stage B. Note absence of Aβ deposition in cases with sAD-related pathology at Stage 0 of Braak and Braak classification. **(B)** Concentrations of Aβ40 and Aβ42 in the entorhinal cortex, orbitofrontal cortex, and frontal cortex area 8 in MA individuals with no sAD-related pathology and in sAD at different stages of Braak and Braak classification. Left: Data are expressed in relation to Stages I–VI of NFT pathology and are presented as mean (SE). * $p < 0.05$, ** $p < 0.01$, *** $p < 0.001$, sAD versus MA cases. $^{\#}$ $p < 0.05$, $^{\#\#}$ $p < 0.01$, sAD V–VI/C versus sAD I–II/0(A). $^{\$}$ $p < 0.05$, $^{\$\$}$ $p < 0.01$, sAD V–VI/C versus sAD III–IV/A–B. Right: Concentrations of Aβ40 and Aβ42 in the same regions, expressed according to Aβ plaque Stages 0, A, B, and C. Data are represented as mean (SE). * $p < 0.05$, ** $p < 0.01$, *** $p < 0.001$, sAD versus MA cases. $^{\#}$ $p < 0.05$, $^{\#\#}$ $p < 0.01$, and $^{\#\#\#}$ $p < 0.001$, Stages A, B, and C versus Stage 0. $^{\$}$ $p < 0.05$, $^{\$\$}$ $p < 0.01$, Stage B or C versus Stage A. **(C)** Representative images of membrane-associated Aβ17–20 in the entorhinal cortex, orbitofrontal cortex, and frontal cortex area 8 in MA individuals with no sAD-related pathology and in sAD at different stages (Stages 0–C) of Braak and Braak classification. Note the absence of membrane-associated Aβ in control brains and in cases with sAD-related pathology at Stage 0 (most with NFT pathology at Stages I–II: 16 of 24; Table 1). Weak expression of membrane-associated Aβ occurs in approximately half of sAD cases at Stage A (representing 4 of 24 cases; Table 1). Expression levels of membrane-associated Aβ17–20 increase with disease progression at Stages B and C. Beta-actin is used as control for protein loading.

become more reactive with aging (67). The present study is the first to identify a particular molecular profile of gene regulation with normal aging in mice and humans, as revealed by a shift in the gene expression of cytokines and mediators of immune response with age. Major changes occur between months 12 and 20/22 in WT mice and in MA individuals without AD-related pathology compared with older individuals at the first stages of sAD-related pathology. Altered regulation of mRNA expression involves a wide range of genes, including members of the complement system, colony-stimulating factor receptors, Toll-like receptors, chemokines, pro-inflammatory cytokines, and anti-inflammatory cytokines, in both rodents and humans. Several observations suggest that systemic inflammation may potentiate neurodegeneration (68–72), but systemic inflammation was specifically ruled out in murine and human cases in this study. Therefore, the present observations show that modifications in the gene regulation of cytokines and mediators of immune response in the brain are indeed manifestations of normal aging.

Modifications in the Gene Regulation of Cytokines and Mediators of Immune Response in APP/PS1 Transgenic Mice Are Reminiscent of, But Are Not Accelerated With, Aging AQ2

Increased mRNA expression of C3ar1, C4b, Csfr3, Tlr7, Ccl3, Ccl4, Ccl6, CxCl10, Il1b, Il6, Tnfα, Il10, Il10rb, and Tgfβ1 was found in WT mice at the age of 20 months, but in APP/PS1 transgenic mice at the age of 12 months. However, the mRNA expression of C1ql1, C1qtnf7, Il6st, Tnfrsf1a, and Il10ra was found to be independent in WT and APP/PS1 mice at the ages of 20/22 and 12 months, respectively. Therefore, inflammation-related gene deregulation in

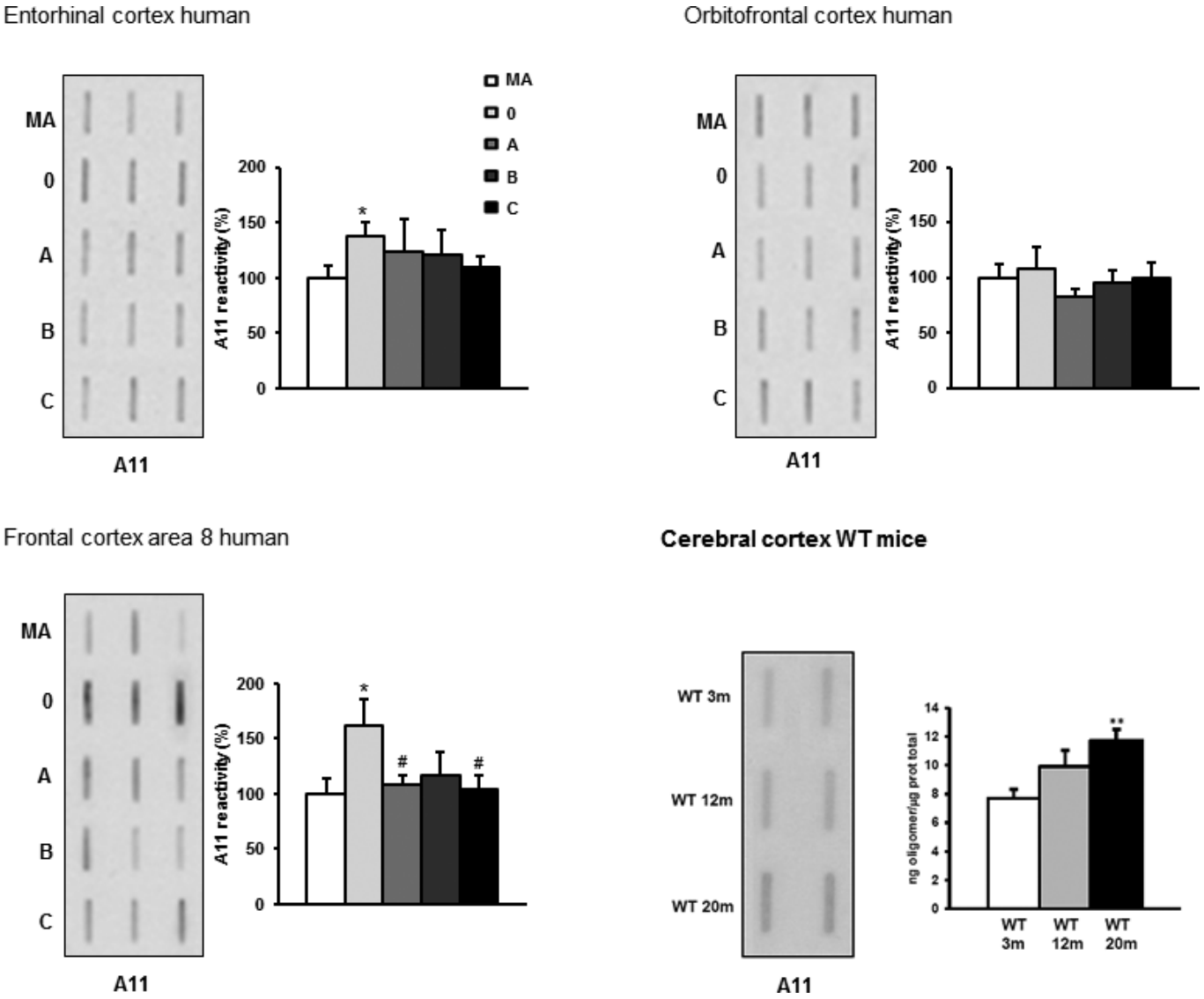

FIGURE 10. Dot blot analysis of soluble oligomers, as revealed by A11 antibody in the entorhinal cortex, orbitofrontal cortex, and frontal cortex area 8 in MA cases and sAD at different stages of Braak and Braak classification (Stages 0, A, B, and C), and in WT mice with age. Data are represented as mean (SE). * $p < 0.05$, significant differences between sAD Stage 0 and middle age. # $p < 0.05$, significant differences between Stages A and C, and Stage 0 (Student *t*-test). A significant increase in the expression levels of soluble oligomers is also seen in the cerebral cortex of WT mice at the age of 20/22 months (20 in the figure) when compared with mice aged 3 and 12 months (Student *t*-test, ** $p < 0.01$).

APP/PS1 transgenic mice involves certain inflammatory mediators that are also abnormally regulated in WT mice with aging. Deregulation of cytokines and mediators of immune response is extensive and much more pronounced in APP/PS1 transgenic mice versus WT mice at any age.

Modifications in the Gene Regulation of Cytokines and Mediators of Immune Response With Aging Are Similar, But Not Identical, in Mice and Humans

Messenger RNA upregulation of cytokines and mediators of immune response in MA individuals with no sAD-related pathology and in individuals with sAD-related pathology at Stages I–II/0–A of Braak and Braak classification involves IL1B, IL6, and IL10 in the entorhinal cortex; IL1B, IL6, IL10, and TLR7 mRNAs in the orbitofrontal cortex; and IL1B, IL6, IL10RA, CSF1R, and TGFβ1 mRNAs in frontal cortex area 8. Expression of Il1b, Il6, Tnfα, Il10, Il10rb, and Tgfβ mRNAs is also upregulated in the cerebral cortex of WT mice at the age of 20/22 months when compared with younger animals, thus suggesting that similar age-related gene responses linked to neuroinflammation occur in mice and humans. However, responses with aging are more extensive in mice than in humans, as mRNAs encoding several members of the complement system, Toll-like receptors, and chemokines are upregulated in mice but not in humans.

Modifications in the Gene Regulation of Cytokines and Mediators of Immune Response Are Similar, But Not Identical, in sAD and APP/PS1 Transgenic Mice

The extent and intensity of the altered regulated gene expression of cytokines and mediators of immune response increase with disease progression in the cerebral cortex of APP/PS1 mice aged 12 months and in the cerebral cortex of AD at Stages III–IV/A–B of Braak and Braak classification. Upregulated mRNA expression involves members of the complement system; colony-stimulating factor receptors; Toll-like receptors; chemokines; IL1B, IL6, IL10, and related receptors; TNFα; and TGFβ1 and TGFβ2. Yet mRNA deregulation differs in sAD and APP/PS1 mice. Thus, Tlr4, Tnfα, and Il10rb mRNAs are abnormally regulated in APP/PS1 mice but not in AD at any stage; and CSF1R, IL6ST, and TGFβ2 mRNAs are abnormally regulated only in frontal cortex area 8 but not in other cortical regions in sAD. These differences, together with the marked regional differences in gene expression in sAD, indicate that neuroinflammation-linked gene expression responses, although similar, are not identical in APP/PS1 mice and sAD. This is not an unexpected observation, as the disease in APP/PS1 mice is reminiscent of, but not identical to, sAD particularly because no NFTs are present in mice. Moreover, species differences also have a role, as can be inferred by the differences in gene expression already discussed in mice and humans with age. These differences may have practical implications when using animal models to test treatments that may be later translated to humans. A summary of similarities and differences between mice and humans is shown in Table 7. T7

Gene Regulation of Cytokines and Mediators of Immune Response Is Modified With the Progression of the Neurodegenerative Process

Although the expression of some genes in APP/PS1 mice is significantly higher at the age of 20/22 months when compared with the age of 12 months, the expression levels of other genes are significantly lower in older animals when compared with APP/PS1 mice aged 12 months. A switch in the characteristics of inflammatory response has also been described in $PS1_{M146L}/APP_{751SL}$ transgenic mice (73). This change of direction has important potential implications because it occurs in the hippocampus by relocation of the alternative (beneficial) activated microglia phenotype at the beginning of Aβ pathology into a classic (cytotoxic) activated microglia phenotype at later stages, together with the expression of pro-inflammatory cytokines and cytotoxic markers at advanced stages of the disease (73). We cannot rule out the possibility that a similar beneficial immune response occurs in APP/PS1 transgenic mice at the age of 6 months (i.e. at the beginning of plaque deposition in the cerebral cortex). However, the expression levels of Il1b, Tnfα C3ar1, C4b, Tlr7, and CxCl10 mRNAs were higher at the age of 20/22 months when compared with transgenic mice aged 12 months. The scenario is complex because Il10 mRNA expression is increased whereas Il10ra, Il10rb, C1qtnf17, Csff1r, Tlr4, Il6st mRNA expression levels are decreased and enhanced Tgfβ1 expression is maintained. Therefore, a sharp distinction between beneficial and cytotoxic inflammatory responses with disease progression is not clear in the cerebral cortex of APP/PS1 transgenic mice at the ages of 12 and 20/22 months. Rather, a combination of pro-inflammatory and anti-inflammatory cytokines and a mixture of beneficial and cytotoxic inflammatory responses seem to be the most realistic scenario at the middle and advanced stages of the disease in APP/PS1 transgenic mice.

Moving to sAD, there is no definite pattern shift (from beneficial to cytotoxic) in the expression of analyzed genes encoding cytokines and mediators of immune response, but rather a tendency—sometimes significant—for decreased gene expression of pro-inflammatory and anti-inflammatory cytokines at Stages V–VI/C when compared with Stages III–IV/A–B of Braak and Braak classification. AQ2

Protein Expression of Selected Cytokines and Mediators in the Cerebral Cortex of APP/PS1 Mice and in the Frontal Cortex in sAD, and Localization in sAD

Western blot analysis of murine cerebral cortex has shown an increase in IL1β and IL6 in WT animals between the ages of 12 and 20/22 months, and in IL1β, IL6, and IL10 in APP/PS1 transgenic mice with disease progression, thus matching corresponding data on mRNA expression.

Protein expression levels of IL1β and IL6 significantly increased at sAD Stages I–II/0 when compared with MA individuals with no AD-related pathology, thus matching corresponding mRNA expression levels. The protein expression

TABLE 7. Similarities and Differences in Gene Expression of Cytokines and Inflammatory Mediators With Aging and AD Progression Between Mice and Humans

	Regulated Cytokines and Mediators (All Upregulated Unless Marked by ↓)
Aging	
WT mice at 12 vs 20/22 months	*C1ql1*, *C3ar1*, *Csf1r*, *Csf3r*, *Tlr4*, *Tlr7*, *Ccl3*, *Ccl4*, *Ccl6*, *CxCl10*, *Il1b*, *Il6*, *Tnf*, *Il10*, *Il10rb*, *Tgfβ2*
Middle age vs AD I–II 0(A)	*CSAR1*, *CSF1R*, *CSF3R*, *TLR7*, *IL1B*, *IL6*, *IL6ST*, *IL10RA*, *TGFβ1*
AD progression	
APP/PS1 at 3 vs 20/22 months	*C1qtnf7*, *C3ar1*, *C4b*, *Csf1r*, *Csf3r*, *Tlr4*, *Tlr7*, *Ccl3*, *Ccl4*, *Ccl6*, *CxCl10*, *Il1b*, *Il6*, *Il6st*, *Tnf*, *Tnfrsf1a*, *Il10*, *Il10ra*, *Il10rb*, *Tgfβ1*
APP/PS1 at 12 months vs APP/PS1 at 20/22 months	*C1qtnf7* (↓), *C3ar1*, *C4b*, *Csf1r* (↓), *Csf3r*, *Tlr4* (↓), *Tlr7*, *CxCl10*, *Il1b*, *Il6st* (↓), *Tnf*, *Il10ra* (↓), *Il10rb* (↓)
AD I–II/0(A) vs AD V–VI/C	*CSAR1*, *CSF1R* (↓), *CSF3R*, *TLR7*, *IL1B* (↓), *IL6* (↓), *IL6ST*, *IL10RA*, *TGFβ1*, *TGFβ2*

patterns match mRNA expression levels with disease progression, although IL6 protein level decreased below MA levels at advanced stages of sAD. However, IL10 protein level markedly increased at Stages V–VI/C, despite the lack of modifications of IL10 mRNA expression.

Increased protein expression levels of cytokines and mediators at advanced stages of sAD are very well documented in a large number of studies and support a consistent and robust core of information considering neuroinflammation as a principal component of sAD pathology (14, 23–41). The novelty of the present observations is that there is a shift in the protein expression of selected cytokines between MA individuals with no sAD-related pathology and individuals with concomitant sAD-related pathology at Stages I–II/0. Importantly, these changes are found in frontal cortex area 8, an area where no NFTs and no Aβ plaques are present at this stage.

Immunohistochemistry has shown that IL6, IL10, TNFα, and NFκB are expressed in ramified microglia in the frontal cortex (and entorhinal cortex) at the first stages of sAD-related pathology. These modifications are, at least in part, a consequence of increased numbers of ramified microglial cells and increased hypertrophy of ramified microglial cells, as revealed by Iba1 immunohistochemistry at early sAD stages. These findings support and expand previous observations showing that so-called microglial dystrophy or senescent microglia (ramified and nonamoeboid) are coincidental with or precede tau pathology in AD (50, 51).

Lack of Relationship Between Aβ Plaques and NFTs, and Gene Regulation of Cytokines and Mediators of Immune Response at the First Stages of sAD

A common line of thinking is derived from the Aβ cascade hypothesis, which postulates that Aβ deposition triggers plaque formation, abnormal tau hyperphosphorylation, oxidative stress, neuroinflammation, and neurodegeneration in AD (74). Although possibly valid in early-onset familial AD, the stringent concept of the Aβ cascade hypothesis does not entirely match the morphologic neuropathology at the first stages of sAD, in which the distribution of Aβ plaques differs from that of NFTs (13, 75). However, these data do not contradict the evidence that Aβ fuels tauopathy in sAD (76–80).

The present observations show no relationship between the modified gene regulation of cytokines and mediators of immune response and Aβ plaques in the early stages of sAD-related pathology; marked modifications occur in the absence of Aβ plaques in the frontal cortex, entorhinal cortex, and, minimally, orbitofrontal cortex, as defined by Stage 0 (16 of 24) and Stage A (8 of 24) of cases with Stages I–II of NFT pathology. Furthermore, analysis of gene expression specifically referring to Aβ plaques stresses a lack of relationship between gene regulation and Aβ plaques at the first stages of sAD-related pathology. Moreover, modifications in the gene expression of cytokines and mediators of immune response are variable from one cortical region to another at the middle stages of sAD, and they do not reflect Aβ plaque burden and NFTs. These findings do not challenge the well-known activation of microglia and astrocytes and the enhanced expression of cytokines and immune mediators triggered in the vicinity of Aβ plaques in AD (1, 14, 24–35, 81); rather, they point to the fact that Aβ plaques do not trigger neuroinflammatory responses at the initial sAD stages.

A few studies have stressed that neuroinflammation may be initiated before plaque deposition in transgenic mouse models (82, 83). This also occurs in APP/PS1 transgenic mice, in which mRNA upregulation of a limited number of members of the complement system, Toll-like receptors, and chemokines of the C-C subfamily occurs at the age of 3 months, when no neurologic deficits are identified and few Aβ deposits, if any, are seen in the cerebral cortex (56).

Aβ40 and Aβ42 Concentrations Do Not Parallel Modifications in the Gene Regulation of Cytokines and Mediators of Immune Response at the First Stages of sAD

The present observations indicate no relationship between concentrations of Aβ40 and Aβ42 and modifications in the gene expression of cytokines and mediators of immune response in the frontal cortex and entorhinal cortex at the first stages of sAD, whereas high concentrations of Aβ40 and Aβ42 correlate with inflammatory gene regulation in all the regions examined at advanced stages of sAD. In contrast to sAD, human Aβ40 and Aβ42 levels are increased in APP/PS1 mice aged 3 months when compared with WT animals, in which no human Aβ can be evidenced, and the expression of human Aβ40 and Aβ42 is markedly increased in APP/PS1 mice aged 6 and 12 months (48). Therefore, human Aβ40 and Aβ42 levels correlate with the gene regulation of cytokines and mediators of immune response in APP/PS1 mice.

Membrane-Associated Aβ Does Not Parallel the Gene Regulation of Cytokines and Mediators of Immune Response at the First Stages of sAD

Membrane-associated Aβ has been postulated as a particular form of Aβ different from soluble and fibrillar Aβ of amyloid plaques, and with potential harmful roles in neurodegeneration in APP transgenic mice and sAD (84, 85). Importantly, membrane-associated Aβ has been found at the early stages of sAD-related pathology and is thus a candidate for explaining the link between Aβ and gene deregulation of cytokines and mediators of immune response at preclinical sAD stages (85). It must be stressed that seminal studies at the early (preclinical) stages of sAD-related pathology included cases with medial temporal Aβ phases 1 and 2 and biochemical stages of Aβ, predominantly 1–3 (only 6 of 19 cases of that series were scored as 0) (85). In contrast, the first stages of sAD in the present series are identified as Stage 0 of plaque burden. No membrane-associated Aβ has been detected in these cases. Moreover, in agreement with the same previous observations (85), membrane-associated Aβ correlates with the presence of fibrillar Aβ in Aβ plaques.

Oligomeric Species

Cumulative evidence supports soluble oligomeric species of Aβ, rather than fibrillar Aβ, as primary Aβ deposits and main causative factors of neuronal damage in sAD (86–94). Amyloid oligomeric species are mainly derived from Aβ42, but they also contain Aβ40, various N-terminal and C-terminal

variants, N-terminal truncated forms, and pyroglutamate Aβ (95–103). Soluble fibrillar oligomer levels are increased in AD brain and correlate with cognitive dysfunction (104). In contrast, soluble oligomer levels have been reported to be similar between controls and sAD cases (96). However, controls in previous studies were aged individuals with sAD-related pathology at Stages I–III without cognitive impairment. The present observations demonstrate that a significant increase in the expression levels of soluble oligomers is found in the entorhinal cortex and frontal cortex area 8 (and a nonsignificant increase in the orbitofrontal cortex) when comparing MA individuals lacking sAD-related pathology with cases with sAD-related pathology at Stages I–II. Therefore, increased levels of soluble oligomers are indeed a characteristic feature of the human aging brain, coincidental with the first stages of AD-related pathology. Because the antibody used (i.e. A11) recognizes amino acid sequence–independent oligomers of proteins or peptides, we cannot ascertain the nature of those soluble oligomers; that means that, in addition to Aβ-derived species, other soluble oligomers can be present in the aging brain, coincidental with the appearance of sAD-related pathology. Whether increased expression of soluble oligomers with aging occurs in other species is here supported by the increased expression levels of soluble oligomers in the cerebral cortex of aged mice (20/22 months old), despite the lack of evidence of any morphologically visible Aβ deposition.

Recent studies have proposed that AD can be triggered by self-produced antigens in brain cells that result in a general autoimmune response facilitated by an impaired blood-brain barrier (105). Whether truncated proteins, lipids, and posttranslationally modified proteins resulting from oxidative and nitrosative damage, in addition to certain Aβ species, can be considered putative self-produced antigens to induce regulation of cytokines and mediators of immune response with aging and sAD needs to be elucidated.

Neuroinflammation and Anti-inflammatory Therapies in sAD: What Is Next?

Classically, increased expression of cytokines and mediators of immune response in the CNS, together with microglial activation, has been interpreted as an indicator of neuroinflammation. On the other hand, other data indicate a much more complex scenario, in which microglia and mediators participate in a large number of processes linked to synaptic development and plasticity, neuronal homeostasis, and pain (44–48, 106–112). In this regard, the present observations, particularly those related to aging and early stages of sAD-related pathology, do not necessarily preclude pathogenic consequences. The different roles of cytokines and mediators have been comprehensibly summarized (23–38), but there is still a large field for the study of their effects in different settings. Whether changes in microglia and altered expression of brain cytokines and inflammatory mediators in the aging brain are protective, damaging, or both cannot be solved with the present data.

In addition to conceptual insights that increase our understanding of the pathogenesis of sAD, the present findings have therapeutic implications. Early administration of anti-inflammatory drugs normalizes cytokine production, reduces brain damage, and prevents cognitive deficits in mouse models reminiscent of AD (113–117). However, anti-inflammatory therapy has no beneficial effect on clinically established AD (25, 118–123). The present observations provide some clues toward explaining such discrepancies: i) treatment in transgenic mice is usually started at the beginning of the neurodegenerative process, whereas treatment in sAD is conducted at advanced stages of the disease, at which time the complexity of inflammatory response is even more complicated by regional differences herein only analyzed in 3 different cortical regions, each one with a particular deregulated pattern; ii) APP/PS1 transgenic mice show different timing of Aβ concentration, deposition of fibrillar forms, and neuroinflammatory responses when compared with humans. Consequently, transgenic mice expressing human *APP* and *PSN1* mutations (at least APP/PS1) seem to be suboptimal models for the analysis of neuroinflammation in sAD or for testing anti-inflammatory therapies applicable to humans; and iii) intrinsic inflammatory-like responses, at least in humans, are complex, and their roles (neuroprotective, damaging, or both) can shift with disease progression at different paces, depending on the region. Whether these capacities depend on the senescent state of microglia (124) needs further study.

However, a large amount of epidemiologic data indicate that anti-inflammatory agents dispensed for therapeutic purposes to patients with autoimmune diseases are protective against sAD (14, 125–132). This proves that rationalized anti-inflammatory therapy can be useful in delaying sAD when acting just before, or perhaps at the same time as, the first stages of sAD-related pathology. Unfortunately, the sensitivity of currently available biomarkers is far from what would be needed to detect the very first stages of sAD. Present findings further support the concept that a therapeutic window exists roughly between the ages of 50 and 65 years, when the first morphologic changes in sAD appear in the brain of a large percentage of clinically normal individuals (13).

On the other hand, the complexity of inflammatory-like responses, largely depending on the stage of the disease and the region involved, stresses that the exact target or targets of anti-inflammatory compounds need to be scrutinized in greater detail and adapted so as to offer advantages with minor or null negative consequences.

CONCLUSIONS

The present findings show that: i) major changes in the brain gene regulation of cytokines and mediators of immune response—some of which are expressed in ramified microglia—occur with aging, which in humans is coincidental with the first alterations of sAD-related pathology; ii) gene deregulation in APP/PS1 transgenic mice and at advanced stages of sAD is not merely nonspecific accelerated aging but rather species-specific and regional- and stage-dependent; iii) in contrast to advanced stages of sAD, the gene regulation of cytokines and mediators of immune response at the first stages of sAD is not related to hyperphosphorylated tau, Aβ plaque burden, concentrations of Aβ40 and Aβ42, and Aβ linked to membranes; however, modification in the expression of cytokines occurs in parallel to the increased expression of

soluble oligomers at the first stages of AD-related pathology; iv) increased levels of soluble oligomers are also observed in the brain of WT mice with age; and v) species differences and region- and stage-dependent inflammatory responses, particularly those occurring at the first stages of sAD, highlight the need to identify new anti-inflammatory compounds adapted to specific molecular targets as complementary treatment in sAD.

ACKNOWLEDGMENTS

The help of R. Gonzalo (Scientific and Technical Support Unit) and E. Vegas and A. Sánchez (Statistics and Bioinformatics Unit, Vall d'Hebrón Research Institute, Barcelona, Spain) is deeply appreciated. We wish to thank T. Yohannan for editorial help.

AQ9

REFERENCES

1. Duyckaerts C, Dickson D. Neuropathology of Alzheimer's disease and its variants. In: Dickson D, Weller R, eds. *Neurodegeneration: The Molecular Pathology of Dementia and Movement Disorders*, 2nd ed. West Sussex, England: Wiley-Blackwell, 2011:62–91
2. Bertram L, Tanzi RE. Genetics of Alzheimer's disease. In: Dickson D, Weller R, eds. *Neurodegeneration: The Molecular Pathology of Dementia and Movement Disorders*, 2nd ed. West Sussex, England: Wiley-Blackwell, 2011:51–61
3. Braak H, Braak E. Neuropathological staging of Alzheimer-related changes. Acta Neuropathol 1991;82:239–59
4. Braak H, Braak E. Frequency of stages of Alzheimer-related lesions in different age categories. Neurobiol Aging 1997;18:351–57
5. Braak H, Braak E. Temporal sequence of Alzheimer's disease–related pathology. In: Peters A, Morrison JH, eds. *Cerebral Cortex: Neurodegenerative and Age-Related Changes in Structure and Function of Cerebral Cortex*, vol. 14. New York, NY: Kluwer Academic/Plenum Publishers, 1999:475–512
6. Braak H, Thal DR, Ghebremedhin E, del Tredici K. Stages of the pathologic process in Alzheimer disease: Age categories from 1 to 100 years. J Neuropathol Exp Neurol 2011;70:960–69
7. Grinberg LT, Rb U, Ferretti RE, Nitrini R, Farfel JM, Polichiso L; Brazilian Brain Bank Study Group. The dorsal raphe nucleus shows phospho-tau neurofibrillary changes before the transentorhinal region in Alzheimer's disease. A precocious onset? Neuropathol Appl Neurobiol 2009;35:406–16
8. Thal DR, Rüb U, Orantes M, Braak H. Phases of Aβ-deposition in the human brain and its relevance for the development of AD. Neurology 2002;58:1791–800
9. Markesbery WR. Neuropathologic alterations in mild cognitive impairment: A review. J Alzheimers Dis 2010;19:221–28
10. Nelson PT, Alafuzoff I, Bigio EH, et al. Correlation of Alzheimer disease neuropathologic changes with cognitive status: A review of the literature. J Neuropathol Exp Neurol 2012;71:362–81
11. Price JL, McKeel DW Jr, Buckles VD, et al. Neuropathology of non-demented aging: Presumptive evidence for preclinical Alzheimer disease. Neurobiol Aging 2009;30:1026–36
12. Ohm TG, Müller H, Braak H, Bohl J. Close-meshed prevalence rates of different stages as a tool to uncover the rate of Alzheimer's disease–related neurofibrillary changes. Neuroscience 1995;64:209–17
13. Ferrer I. Defining Alzheimer as a common age-related neurodegenerative process not inevitably leading to dementia. Prog Neurobiol 2012; 97:38–51
14. McGeer PL, McGeer EG. The amyloid cascade—inflammatory hypothesis of Alzheimer disease: Implications for therapy. Acta Neuropathol 2013;126:479–97
15. Selkoe DJ. Preventing Alzheimer's disease. Science 2012;337:1488–92
16. Ferrer I. Altered mitochondria, energy metabolism, voltage-dependent anion channel, and lipid rafts converge to exhaust neurons in Alzheimer's disease. J Bioenerg Biomembr 2009;41:425–31
17. Pamplona R, Dalfó E, Ayala V, et al. Proteins in human brain cortex are modified by oxidation, glycoxidation, and lipoxidation: Effects of Alzheimer disease and identification of lipoxidation targets. Mol J Biol Chem 2005;1280:21522–30
18. Sultana R, Butterfield DA. Role of oxidative stress in the progression of Alzheimer's disease. J Alzheimers Dis 2010;19:341–53
19. Martín V, Fabelo N, Santpere G, et al. Lipid alterations in lipid rafts from Alzheimer's disease human brain cortex. J Alzheimers Dis 2010; 19:489–502
20. Cataldo AM, Paskevich PA, Kominami E, Nixon RA. Lysosomal hydrolases of different classes are abnormally distributed in brains of patients with Alzheimer disease. Proc Natl Acad Sci U S A 1991;88: 10998–1002
21. Keller JN, Hanni KB, Markesbery WR. Impaired proteasome function in Alzheimer's disease. J Neurochem 2000;75:436–39
22. Heneka MT, Kummer MP, Latz E. Innate immune activation in neurodegenerative disease. Nat Rev Immunol 2014;14:463–77
23. Mc Geer PL, McGeer EG. The inflammatory response system of brain: Implications for therapy of Alzheimer and other neurodegenerative diseases. Brain Res Rev 1995;21:195–218
24. McGeer PL, McGeer EG. History of innate immunity in neurodegenerative disorders. Front Pharmacol 2011;2:77
25. Moore AH, O'Banion MK. Neuroinflammation and anti-inflammatory therapy for Alzheimer's disease. Adv Drug Deliv Rev 2002;54:1627–56
26. Prokop S, Miller KR, Heppner FL. Microglia actions in Alzheimer's disease. Acta Neuropathol 2013;126:461–77
27. Aisen PS, Davis KL. Inflammatory mechanisms in Alzheimer's disease. Am J Psychiatry 1994;151:1105–13
28. Neurobiol Aging 1996;17 (special issue) AQ10
29. Roggers J, Griffin WST. Inflammatory mechanisms of Alzheimer's disease. In: Wood PL, ed. *Neuroinflammation: Mechanisms and Management*. Totowa, NY: Humana Press, 1998:177–93
30. Arends YM, Duyckaerts C, Rozemuller JM, et al. Microglia, amyloid and dementia in Alzheimer's disease. A correlative study. Neurobiol Aging 2000;21:39–47
31. Bamberger ME, Harris ME, McDonald DR, et al. A cell surface receptor complex for fibrillary-amyloid mediates microglial activation. J Neurosci 2003;23:2665–74
32. McGeer PL, McGeer EG. Inflammation and the degenerative diseases of aging. Ann N Y Acad Sci 2004;1035:104–16
33. Weller RO, Subash M, Preston SD, et al. Perivascular drainage of amyloid-beta peptides from the brain and its failure in cerebral amyloid angiopathy and Alzheimer's disease. Brain Pathol 2008;18:253–66
34. Mandrekar S, Jiang Q, Lee CY, et al. Microglia mediate the clearance of soluble Abeta through fluid phase macropinocytosis. J Neurosci 2009; 29:4252–62
35. Akiyama H, Barger S, Barnum S, et al. Inflammation and Alzheimer's disease. Neurobiol Aging 2000;21:383–421
36. Lee YJ, Han SB, Nam SY, Oh KW, Hong JT. Inflammation and Alzheimer's disease. Arch Pharm Res 2010;33:1539–56
37. McGeer PL, McGeer EG. Inflammation, autotoxicity and Alzheimer disease. Neurobiol Aging 2001;22:799–809
38. Rubio-Perez JM, Morillas-Ruiz JM. A review: Inflammatory process in Alzheimer's disease, role of cytokines. Sci World J 2012;2012:56357
39. Streit WJ, Conde JR, Harrison JK. Chemokines and Alzheimer's disease. Neurobiol Aging 2001;22:909–13
40. Matsuoka Y, Picciano M, Malester B, et al. Inflammatory responses to amyloidosis in a transgenic mouse model of Alzheimer's disease. Am J Pathol 2001;158:1345–54
41. Wirz KTS, Bossers K, Stargardt A, et al. Cortical beta-amyloid protein triggers an immune response, but not synaptic changes in the APPswe/PS1dE9 Alzheimer's disease mouse model. Neurobiol Aging 2013:34:1328–42
42. Griffin WS, Sheng JG, Royston MC, et al. . Glial-neuronal interactions in Alzheimer's disease: The potential role of a 'cytokine cycle' in disease progression. Brain Pathol 1998;8:65–72
43. Leung E, Guo L, Bu J, et al. Microglia activation mediates fibrillar amyloid-beta toxicity in the aged primate cortex. Neurobiol Aging 2011;32:387–97
44. Streit WJ, Greber MB, Kreutzberg GW. Functional plasticity of microglia: A review. Glia 1988;1:301–7
45. Kreutzberg GW. Microglia: A sensor for pathological events in the CNS. Trends Neurosci 1996;19:312–18

46. Streit W. Microglia and neuroprotection: Implications for Alzheimer's disease. Brain Res Rev 2005;48:234–39
47. Graeber MB, Streit WJ. Microglia: Biology and pathology. Acta Neuropathol 2010;119:89–105
48. Graeber MB, Li W, Michael L, Rodríguez ML. Role of microglia in CNS inflammation. FEBS Lett 2011;585:3798–805
49. Morimoto K, Horio J, Satoh H, et al. Expression profiles of cytokines in the brains of Alzheimer's disease (AD) patients, compared to the brains of non-demented patients with and without increasing AD pathology. J Alzheimers Dis 2011;25:59–76
50. Streit WJ, Samkons NW, Kuhns AJ, Sparks DL. Dystrophic microglia in the aging human brain. Glia 2004;45:208–12
51. Streit WJ, Braak H, Xue QS, et al. Dystrophic (senescent) rather than activated microglial cells are associated tau pathology and likely precede neurodegeneration in Alzheimer's disease. Acta Neuropathol 2009; 118:475–85
52. Fernández PL, Britton GB, Rao KS. Potential immunotargets of Alzheimer's disease treatment strategies. J Alzheimers Dis 2013;33: 297–312
53. McGeer EG, McGeer PL. Neuroinflammation in Alzheimer's disease and mild cognitive impairment: A field in its infancy. J Alzheimers Dis 2010;19:355–61
54. Li C, Ebrahimi A, Schluesener H. Drug pipeline in neurodegeneration based on transgenic mice models of Alzheimer's disease. Ageing Res Rev 2013;12:116–40
55. Borchelt DR, Thinakaran G, Eckman CB, et al. Familial Alzheimer's disease–linked presenilin 1 variants elevate Abeta1–42/1–40 ratio in vitro and in vivo. Neuron 1996;17:1005–13
56. Aso E, Lomoio S, López-González I, et al. Amyloid generation and dysfunctional immunoproteasome activation with disease progression in animal model of familial Alzheimer's disease. Brain Pathol 2012;22: 636–53
57. Braak H, Alafuzoff I, Arzberger T, et al. Staging of Alzheimer disease–associated neurofibrillary pathology using paraffin sections and immunocytochemistry. Acta Neuropathol 2006;112:389–404
58. Gentleman RC, Carey VJ, Bates DM, et al. Bioconductor: Open software development for computational biology and bioinformatics. Genome Biol 2004;5:R80
59. Smyth GK. Machine learning concepts and tools for statistical genomics. In: Gentleman R, Carey V, Dudoit S, Irizarry R, Huber W, eds. *Bioinformatics and Computational Biology Solutions Using R and Bioconductor*. New York, NY: Springer, 2005:397–420
60. Schlüter A, Espinosa L, Fourcade S, et al. Functional genomic analysis unravels a metabolic-inflammatory interplay in adrenoleukodystrophy. Hum Mol Genet 2012;21:1062–77
61. Falcon S, Gentleman R. Using GOstats to test gene lists for GO term association. Bioinformatics 2007;23:257–58
62. Mootha VK, Bunkenborg J, Olsen JV, et al. Integrated analysis of protein composition, tissue diversity, and gene regulation in mouse mitochondria. Cell 2003;115:629–40
63. Barrachina M, Castaño E, Ferrer I. TaqMan PCR assay in the control of RNA normalization in human post-mortem brain tissue. Neurochem Int 2006;49:276–84
64. Durrenberg PF, Fernando S, Kashefi SN, et al. Selection of novel reference genes for use in the human central nervous system: A BrainNet Study. Acta Neuropathol 2012;124:893–903
65. Michaud M, Balardy L, Moulis G, et al. Pro-inflammatory cytokines, aging, and age-related diseases. J Am Med Dir Assoc 2013;14:877–82
66. Pizza V, Agresta A, D'Acunto CW, Festa M, Capasso A. Neuroinflammation and ageing: Current theories and an overview of the data. Rev Recent Clin Trials 2011;6:189–203
67. Godbout JP, Johnson RW. Age and neuroinflammation: A lifetime of psychoneuroimmune consequences. Neurol Clin 2006;24:521–38
68. Bodles AM, Barger SW. Cytokines and the aging brain—what we don't know might help us. Trends Neurosci 2004;27:621–26
69. Holmes C. Review: Systemic inflammation and Alzheimer's disease. Neuropathol Appl Neurobiol 2013;39:51–68
70. Ownby RL. Neuroinflammation and cognitive aging. Curr Psychiatry Rep 2010;12:39–45
71. Perry VH. Contribution of systemic inflammation to chronic neurodegeneration. Acta Neuropathol 2010;120:277–86
72. Sardi F, Fassina L, Venturini L, et al. Alzheimer's disease, autoimmunity and inflammation: The good, the bad and the ugly. Autoimmun Rev 2011;11:149–53
73. Jimenez S, Baglietto-Vargas D, Caballero C, et al. Inflammatory response in the hippocampus of mouse model of Alzheimer's disease: Age-dependent switch in the microglial phenotype from alternative to classic. J Neurosci 2008;28:1650–61
74. Hardy J. The amyloid hypothesis for Alzheimer's disease: A critical reappraisal. J Neurochem 2009;110:1129–34
75. Katsuno T, Morishima-Kawashima M, Saito Y, et al. Independent accumulations of tau and amyloid-beta protein in the human entorhinal cortex. Neurology 2005;64:687–82
76. Delacourte A. The natural and molecular history of Alzheimer's disease. J Alzheimers Dis 2006;9:187–84
77. Hurtado DE, Molina-Porcel L, Iba M, et al. Aβ accelerates the spatiotemporal progression of tau pathology and augments tau amyloidosis in an Alzheimer mouse model. Am J Pathol 2010;177:1977–88
78. Lewis J, Dickson DW, Lin WL, et al. Enhanced neurofibrillary degeneration in transgenic mice expressing mutant tau and APP. Science 2001;293:1487–91
79. Masters CL, Beyreuther K. Alzheimer's centennial legacy: Prospects for rational therapeutic intervention targeting the Aβ amyloid pathway. Brain 2006;129:2823–39
80. Tomiyama T, Matsuyama S, Iso H, et al. A mouse model of amyloid beta oligomers: Their contribution to synaptic alteration, abnormal tau phosphorylation, glial activation, and neuronal loss in vivo. J Neurosci 2010;30:4845–56
81. Medeiros R, LaFerla FM. Astrocytes: Conductors of the Alzheimer disease neuroinflammatory symphony. Exp Neurol 2013;239:133–38
82. Ferretti MT, Cuello AC. Does a pro-inflammatory process precede Alzheimer's disease and mild cognitive impairment? Curr Alzheimer Res 2011;8:164–74
83. Yu D, Corbett B, Yan Y, et al. Early cerebrovascular inflammation in a transgenic mouse model of Alzheimer's disease. Neurobiol Aging 2012; 33:2942–47
84. Rijal-Upadhaya A, Capetillo-Zarate E, Kosterin I, et al. Dispersible amyloid β-protein oligomers, protofibrils, and fibrils represent diffusible but not soluble aggregates: Their role in neurodegeneration in amyloid precursor protein (APP) transgenic mice. Neurobiol Aging 2012; 33:2641–60
85. Rijal-Upadhaya A, Kosterin I, Kumar S, et al. Biochemical stages of amyloid-β peptide aggregation and accumulation in the human brain and their association with symptomatic and pathologically preclinical Alzheimer's disease. Brain 2014;137:887–903
86. Haass J, Selkoe DJ. Soluble protein oligomers in neurodegeneration: Lessons from the Alzheimer's amyloid beta-peptide. Nat Rev Mol Cell Biol 2007;8:101–2
87. Glabe CG. Structural classification of toxic amyloid oligomers. J Biol Chem 2008;283:29639–43
88. Glabe CG. Amyloid oligomer structures and toxicity. Open Biol J 2009; 2:222–27
89. Shankar GM, Li S, Mehta TH, et al. Amyloid β-protein dimers isolated directly from Alzheimer brains impair synaptic plasticity and memory. Nat Med 2008;14:837–42
90. Roychaudhuri R, Yang M, Hoshi MM, Teplow DB. Amyloid β-protein assembly and Alzheimer disease. J Biol Chem 2009;284:4749–53
91. Benilova I, Karran T, De Strooper B. The toxic Aβ oligomer and Alzheimer's disease: An emperor in need of clothes. Nat Neurosci 2012; 15:349–57
92. Mucke L, Selkoe DJ. Neurotoxicity of amyloid β-protein: Synaptic and network dysfunction. Cold Spring Harb Perspect Med 2012;2:a006338
93. Zhao LN, Long HW, Mu Y, Chew LY. The toxicity of amyloid β oligomers. Int J Mol Sci 2012;13:7303–27
94. Kayed R, Lasagna-Reeves AL. Molecular mechanisms of amyloid oligomers toxicity. J Alzheimers Dis 2013;33:S67–78
95. Prelli F, Castaño E, Glenner GG, Frangione B. Differences between vascular and plaque core amyloid in Alzheimer's disease. J Neurochem 1988;51:648–51
96. Miller DL, Papayannopoulos IA, Styles J, et al. Peptide compositions of the cerebrovascular and senile plaque core amyloid deposits of Alzheimer's disease. Arch Biochem Biophys 1993;301:41–52

97. Roher AE, Lowenson JD, Clarke S, et al. β-Amyloid-(1–42) is a major component of cerebrovascular amyloid deposits: Implications for the pathology of Alzheimer disease. Proc Natl Acad Sci U S A 1993;90: 10836–40
98. Näslund J, Schierhorn A, Hellman U, et al. Relative abundance of Alzheimer A beta amyloid peptide variants in Alzheimer disease and normal aging. Proc Natl Acad Sci U S A 1994;91:8378–82
99. Saido TC, Iwatsubo T, Mann DM, et al. Dominant and differential deposition of distinct beta-amyloid peptide species, A beta N3(pE), in senile plaques. Neuron 1995;14:457–66
100. Lewis H, Beher D, Cookson N, et al. Quantification of Alzheimer pathology in ageing and dementia: Age-related accumulation of amyloid-beta(42) peptide in vascular dementia. Neuropathol Appl Neurobiol 2006;32:103–18
101. Portelius E, Bogdanovic N, Gustavsson MK, et al. Mass spectrometric characterization of brain amyloid beta isoform signatures in familial and sporadic Alzheimer's disease. Acta Neuropathol 2010;120:185–93
102. Saito T, Suemoto T, Brouwers N, et al. Potent amyloidogenicity and pathogenicity of Aβ43. Nat Neurosci 2011;14:1023–32
103. Jawhar S, Wirths O, Bayer TA. Pyroglutamate amyloid-β (Aβ): A hatched man in Alzheimer disease. J Biol Chem 2011;286:38825–27
104. Tomic JL, Pensalfini A, Head E, Glabe CG. Soluble fibrillar oligomer levels are elevated in Alzheimer's disease brain and correlate with cognitive dysfunction. Neurobiol Dis 2009;35:352–58
105. Arshavsky YI. Alzheimer disease and cellular mechanisms of memory storage. J Neuropathol Exp Neurol 2014;73:192–205
106. Graeber MB. Changing face of microglia. Science 2010;330:783–88
107. Paolicelli RC, Bolasco G, Pagani F, et al. Synaptic pruning by microglia is necessary for normal brain development. Science 2011;333:1456–58
108. Schafer DP, Lehrman EK, Kautzman AG, et al. Microglia sculpt postnatal neural circuits in an activity and complement-dependent manner. Neuron 2012;74:691–705
109. Parkhurst CN, Yang G, Ninan I, et al. Microglia promote learning-dependent synapse formation through brain-derived neurotrophic factor. Cell 2013;155:1596–609
110. Zhan Y, Paolicelli RC, Sforazzini F, et al. Deficient neuron-microglia signaling results in impaired functional brain connectivity and social behavior. Nat Neurosci 2014;17:400–6
111. Estes ML, McAllister AK. Alterations in immune cells and mediators in the brain: It's not always neuroinflammation! Brain Pathol 2014;24: 623–30
112. Svahn AJ, Becker TS, Graeber MB. Emergent properties of microglia. Brain Pathol 2014;24:665–70
113. Lim GP, Yang F, Chu T, et al. Ibuprofen suppresses plaque pathology and inflammation in a mouse model for Alzheimer's disease. J Neurosci 2000;20:5709–14
114. Jantzen PT, Connor KE, DiCarlo G, et al. Microglial activation and beta-amyloid deposit reduction caused by a nitric oxide–releasing nonsteroidal anti-inflammatory drug in amyloid precursor protein plus presenilin-1 transgenic mice. J Neurosci 2002;22:2246–54
115. van Groen T, Miettinen P, Kadish I. Transgenic AD model mice, effects of potential anti-AD treatments on inflammation, and pathology. J Alzheimers Dis 2011;24:301–13
116. Bachstetter AD, Norris CM, Sompol P, et al. Early stage drug treatment that normalizes pro-inflammatory cytokine production attenuates synaptic dysfunction in a mouse model that exhibits age-dependent progression of Alzheimer's disease–related pathology. J Neurosci 2012;32: 10201–10
117. Gabbita SP, Srivastava MK, Eslami P, et al. Early intervention with a small molecule inhibitor for tumor necrosis factor-α prevents cognitive deficits in a triple transgenic mouse model of Alzheimer's disease. J Neuroinflammation 2012;9:99
118. Aisen PS. The potential of anti-inflammatory drugs for the treatment of Alzheimer's disease. Lancet Neurol 2002;1:937–44
119. Reines SA, Block GA, Morris JC, et al. Rofecoxib: No effect on Alzheimer's disease in a 1-year, randomized, blinded, controlled study. Neurology 2004;62:66–71
120. ADAPT Research Group. Cardiovascular and cerebrovascular events in the randomized, controlled Alzheimer's Disease Anti-Inflammatory Prevention Trial (ADAPT). PLoS Clin Trials 2006;1:e33
121. Soininen H, West C, Robbins J, et al. Long-term efficacy and safety of celecoxib in Alzheimer's disease. Dement Geriatr Cogn Disord 2007; 23:8–21
122. Jaturapatporn D, Isaac MG, McCleery J, et al. Aspirin, steroidal and non-steroidal anti-inflammatory drugs for the treatment of Alzheimer's disease. Cochrane Database Syst Rev 2012;2:CD006378
123. Shi S, Wang Z, Qiao Z. The multifunctional anti-inflammatory drugs used in the therapy of Alzheimer's disease. Curr Med Chem 2013;20: 2583–88
124. Streit WJ. Microglial senescence: Does the brain's immune system have an expiration date? Trends Neurosci 2006;29:506–10
125. Mackenzie IRA, Muñoz DG. Non-steroidal anti-inflammatory drug use and Alzheimer-type pathology in aging. Neurology 1998;50:986–90
126. Jenkinson ML, Bliss MR, Brain AT, Scott DL. Rheumatoid arthritis and senile dementia of the Alzheimer's type. Br J Rheumatol 1989;28:86–88
127. McGeer PL, McGeer E, Rogers J, Sibley J. Anti-inflammatory drugs and Alzheimer disease. Lancet 1990;335:1037
128. Myllykangas-Luosujarvi R, Isomaki H. Alzheimer's disease and rheumatoid arthritis. Br J Rheumatol 1994;33:501–2
129. Breitner JC, Welsh KA, Helms MJ, et al. Delayed onset of Alzheimer's disease with non-steroidal anti-inflammatory and histamine H2 blocking drugs. Neurobiol Aging 1995;16:523–30
130. Stewart WF, Kawas C, Corrada M, Metter EJ. Risk of Alzheimer's disease and duration of NSAID use. Neurology 1997;48:626–32
131. Vlad SC, Miller DR, Kowall NW, Felson DT. Protective effects of NSAIDs on the development of Alzheimer disease. Neurology 2008;70: 1672–77
132. Zandi PP, Anthony JC, Hayden KM, et al. Reduced incidence of AD with NSAID but not H2 receptor antagonists: The Cache County Study. Neurology 2002;59:880–86

AUTHOR QUERIES

AUTHOR PLEASE ANSWER ALL QUERIES

AQ1 = Please check affiliations.

AQ2 = Correct as edited?

AQ3 = Original running head exceeded 50 characters and was thus modified. Please check.

AQ4 = Please spell out RIN.

AQ5 = Please spell out MES.

AQ6 = Casing of terms (e.g. CSF1R vs Csf1r) was retained. Please check all occurrences.

AQ7 = Originally $$. Correct as edited?

AQ8 = Please supply legend to footnote ‡‡ (originally $).

AQ9 = Original Refs. 25 and 119 were identical. The latter was deleted and the references were renumbered. Please check.

AQ10 = Please supply author names, article title, and page range.

END OF AUTHOR QUERIES

Author Reprints

For *Rapid Ordering* go to: www.lww.com/periodicals/author-reprints

Journal of Neuropathology & Experimental Neurology

Order

Author(s) Name

Title of Article

*Article # *Publication Mo/Yr

**Fields may be left blank if order is placed before article number and publication month are assigned.*

Quantity of Reprints ____ $_____

Covers (Optional) _____ $_____

Shipping Cost $_____

Reprint Color Cost $_____

Tax $_____

Total $_____

REPRINTS ORDERED & PURCHASED UNDER THE AUTHOR REPRINTS PROGRAM MAY NOT BE USED FOR COMMERCIAL PURPOSES

Reprint Pricing

50 copies = $336.00
100 copies = $420.00
200 copies = $494.00
300 copies = $571.00
400 copies = $655.00
500 copies = $732.00

Plain Covers

$108.00 for first 100 copies
$18.00 each add'l 100 copies

Reprint Color

($70.00/100 reprints)

Shipping

Within the U.S. - $15.00 up to the first 100 copies and $15.00 for each additional 100 copies

Outside the U.S. - $30.00 up to the first 100 copies and $30.00 for each additional 100 copies

Tax

U.S. and Canadian residents add the appropriate tax or submit a tax exempt form.

Payment

● MC ● VISA ● Discover ● American Express

Account # / / Exp. Date

Name

Address Dept/Rm

City State Zip Country

Telephone

Signature

Ship to

Name

Address Dept/Rm

City State Zip Country

Telephone

Lippincott Williams & Wilkins
a Wolters Kluwer business

Use this form to order reprints. Publication fees, including color separation charges and page charges will be billed separately, if applicable.

Payment must be received before reprints can be shipped. Payment is accepted in the form of a check or credit card; purchase orders are accepted for orders billed to a U.S. address.

Prices are subject to change without notice.

For quantities over 500 copies contact our Healthcare Dept. For orders shipping in the US and Canada: call 410-528-4396, fax your order to 410-528-4264 or email it to Meredith.Doviak@wolterskluwer.com. Outside the US: dial 44 1829 772756, fax your order to 44 1829 770330 or email it to Christopher.Bassett@wolterskluwer.com.

MAIL your order to:
Lippincott Williams & Wilkins
Author Reprints Dept.
351 W. Camden St.
Baltimore, MD 21201

FAX:
410.528.4434

For questions regarding reprints or publication fees,
E-MAIL:
reprints@lww.com

OR **PHONE:**
1.866.903.6951

For *Rapid Ordering* go to: www.lww.com/periodicals/author-reprints